siRNA (Dharmacon, Chicago, IL, USA) by using Lipofect AMINE RNAiMAX transfection reagent (Invitrogen) according to the manufacturer's instructions. Forty-eight hours after transfection, total RNA was prepared and subjected to RT–PCR.

Colony formation assay

H1299, SH-SY5Y, U2OS and SAOS-2 cells were seeded at a final density of 1×10^5 cells per six-well dish and allowed to attach overnight. Cells were then co-transfected with the indicated combinations of the expression plasmids. Total amount of plasmid DNA per transfection was kept constant (2 μg) with pcDNA3. Forty-eight hours after transfection, cells were transferred to the fresh medium containing G418 (400 μg ml^{-1}). After 14 days, viable colonies were washed in phosphate-buffered saline and stained with Giemsa's solution.

Acknowledgements

We are grateful to Dr T Kamijo (Division of Biochemistry, Chiba Cancer Center Research Institute) for his helpful discussion. This work was supported in part by a grant-in-aid from the Ministry of Health, Labour and Welfare for Third Term Comprehensive Control Research for Cancer, a grant-in-aid for Scientific Research on Priority Areas from the Ministry of Education, Culture, Sports, Science and Technology, Japan, a grant-in-aid for Scientific Research from Japan Society for the Promotion of Science and Uehara Memorial Foundation.

References

Adhikary S, Marinoni F, Hock A, Hulleman E, Popov N, Beier R *et al.* (2005). The ubiquitin ligase HectH9 regulates transcriptional activation by Myc and is essential for tumor cell proliferation. *Cell* **123**: 409 421.

Bijur GN, De Sarno P, Jope RS. (2000). Glycogen synthase kinase-3beta facilitates staurosporine- and heat shock-induced apoptosis. *J Biol Chem* **275**: 7583 7590.

Cluskey S, Ramsden DB. (2001). Mechanisms of neurodegeneration in amyotrophic lateral sclerosis. *Mol Pathol* **54**: 386 392.

Cross DA, Culbert AA, Chalmers KA, Facci L, Skaper SD, Reith AD. (2001). Selective small-molecule inhibitors of glycogen synthase kinase-3 activity protect primary neurones from death. *J Neurochem* **77**: 94 102.

Di Lello P, Jenkins LM, Jones TN, Nguyen BD, Hara T, Yamaguchi H *et al.* (2006). Structure of the Tfb1/p53 complex: Insights into the interaction between the p62/Tfb1 subunit of TFIIH and the activation domain of p53. *Mol Cell* **22**: 731 740.

Donehower LA, Harvey M, Slagle BL, McArthur MJ, Montgomery Jr CA, Butel JS *et al.* (1992). Mice deficient for p53 are developmentally normal but susceptible to spontaneous tumours. *Nature* **356**: 215 221.

Ekegren T, Grundstrom E, Lindholm D, Aquilonius SM. (1999). Upregulation of Bax protein and increased DNA degradation in ALS spinal cord motor neurons. *Acta Neurol Scand* **100**: 317 321.

Gonzalez de Aguilar JL, Gordon JW, Rene F, de Tapia M, Lutz-Bucher B, Gaiddon C *et al.* (2000). Alteration of the Bcl-x/Bax ratio in a transgenic mouse model of amyotrophic lateral sclerosis: evidence for the implication of the p53 signaling pathway. *Neurobiol Dis* **7**: 406 415.

Hetman M, Cavanaugh JE, Kimelman D, Xia Z. (2000). Role of glycogen synthase kinase-3beta in neuronal apoptosis induced by trophic withdrawal. *J Neurosci* **20**: 2567 2574.

Hino S, Michiue T, Asashima M, Kikuchi A. (2003). Casein kinase I epsilon enhances the binding of Dvl-1 to Frat-1 and is essential for Wnt-3a-induced accumulation of beta-catenin. *J Biol Chem* **278**: 14066 14073.

Hollstein M, Sidransky D, Vogelstein B, Harris CC. (1991). p53 mutations in human cancers. *Science* **253**: 49 53.

Hupp TR, Lane DP. (1994). Regulation of the cryptic sequence-specific DNA-binding function of p53 by protein kinases. *Cold Spring Harb Symp Quant Biol* **59**: 195 206.

Kiryo-Seo S, Hirayama T, Kato R, Kiyama H. (2005). Noxa is a critical mediator of p53-dependent motor neuron death after nerve injury in adult mouse. *J Neurosci* **25**: 1442 1447.

Kishida M, Hino S, Michiue T, Yamamoto H, Kishida S, Fukui A *et al.* (2001). Synergistic activation of the Wnt signaling pathway by Dvl and casein kinase Iepsilon. *J Biol Chem* **276**: 33147 33155.

Kitanaka C, Kato K, Ijiri R, Sakurada K, Tomiyama A, Noguchi K *et al.* (2002). Increased Ras expression and caspase-independent neuroblastoma cell death: possible mechanism of spontaneous neuroblastoma regression. *J Natl Cancer Inst* **94**: 358 368.

Lee E, Salic A, Kirschner MW. (2001). Physiological regulation of [beta]- catenin stability by Tcf3 and CK1epsilon. *J Cell Biol* **154**: 983 993.

Levine AJ, Chang A, Dittmer D, Notterman DA, Silver A, Thorn K *et al.* (1994). The p53 tumor suppressor gene. *J Lab Clin Med* **123**: 817 823.

Martin LJ. (2000). p53 is abnormally elevated and active in the CNS of patients with amyotrophic lateral sclerosis. *Neurobiol Dis* **7**: 613 622.

Martin LJ, Liu Z. (2002). Injury-induced spinal motor neuron apoptosis is preceded by DNA single-strand breaks and is p53- and bax-dependent. *J Neurobiol* **5**: 181 197.

Miyazaki K, Fujita T, Ozaki T, Kato C, Kurose Y, Sakamoto M *et al.* (2004). NEDL1, a novel ubiquitin-protein isopeptide ligase for dishevelled-1, targets mutant superoxide dismutase-1. *J Biol Chem* **279**: 11327 11335.

Miyazaki K, Ozaki T, Kato C, Hanamoto T, Fujita T, Irino S *et al.* (2003). A novel HECT-type E3 ubiquitin ligase, NEDL2, stabilizes p73 and enhances its transcriptional activity. *Biochem Biophys Res Commun* **308**: 106 113.

Moll UM, LaQuaglia M, Benard J, Riou G. (1995). Wild-type p53 protein undergoes cytoplasmic sequestration in undifferentiated neuroblastomas but not in differentiated tumors. *Proc Natl Acad Sci USA* **92**: 4407 44011.

Nakagawara A, Ohira M. (2004). Comprehensive genomics linking between neural development and cancer: neuroblastoma as a model. *Cancer Lett* **204**: 213 224.

Pietenpol JA, Tokino T, Thiagalingam S, el-Deiry WS, Kinzler KW, Vogelstein B. (1994). Sequence-specific transcriptional activation is essential for growth suppression by p53. *Proc Natl Acad Sci USA* **91**: 1998 2002.

Roos WP, Kaina B. (2006). DNA damage-induced cell death by apoptosis. *Trends Mol Med* **12**: 440 450.

Shaw P, Freeman J, Bovey R, Iggo R. (1996). Regulation of specific DNA binding by p53: evidence for a role for *O*-glycosylation and charged residues at the carboxy-terminus. *Oncogene* **12**: 921 930.

Thomas MC, Chiang CM. (2005). E6 oncoprotein represses p53-dependent gene activation via inhibition of protein acetylation independently of inducing p53 degradation. *Mol Cell* **17**: 251 264.

Vousden KH, Lu X. (2002). Live or let die: the cell's response to p53. *Nat Rev Cancer* **2**: 594 604.

Watcharasit P, Bijur GN, Zmijewski JW, Song L, Zmijewska A, Chen X *et al.* (2002). Direct, activating interaction between glycogen synthase kinase-3beta and p53 after DNA damage. *Proc Natl Acad Sci USA* **99**: 7951 7955.

Supplementary Information accompanies the paper on the Oncogene website (http://www.nature.com/onc).

Biochemical and Biophysical Research Communications 369 (2008) 994–1000

Contents lists available at ScienceDirect

Biochemical and Biophysical Research Communications

journal homepage: www.elsevier.com/locate/ybbrc

ΔNp63/BMP-7-dependent expression of matrilin-2 is involved in keratinocyte migration in response to wounding

Tomoe Ichikawa [a,b], Yusuke Suenaga [a,c], Tadayuki Koda [b], Toshinori Ozaki [a,c], Akira Nakagawara [a,c,*]

[a] Division of Biochemistry, Chiba Cancer Center Research Institute, 666-2 Nitona, Chuoh-ku, Chiba 260-8717, Japan
[b] Research Center for Functional Genomics, Hisamitsu Pharmaceutical Co., Inc., Chiba 260-8717, Japan
[c] Department of Molecular Biology and Oncology, Chiba University Graduate School of Medicine, Chiba 260-8717, Japan

ARTICLE INFO

Article history:
Received 20 February 2008
Available online 6 March 2008

Keywords:
BMP-7
ΔNp63
Matrilin-2
Keratinocyte
Migration
Wound healing

ABSTRACT

p63 is expressed as multiple variants including TA and ΔN forms. Since *p63*-deficient mice displayed profound defects of stratified epithelia, p63 is an essential transcription factor required for epidermal morphogenesis. However, precise molecular mechanisms behind contribution of p63 to normal skin formation and healing skin wounds remained unclear. In this study, we demonstrated that ΔNp63/BMP-7 signaling pathway modulates wound healing process through the regulation of extracellular matrix protein matrilin-2. Knocking down of ΔNp63 in human keratinocyte HaCaT cells led to a significant reduction of *matrilin-2*. Intriguingly, BMP-7 which is one of ΔNp63-target gene products, induced *matrilin-2* and attenuated inhibitory effect of siRNA against ΔNp63 on *matrilin-2*. Furthermore, a remarkable cell migration in response to wounding took place in ΔNp63- or matrilin-2-knocked down cells. Taken together, our present findings indicate that ΔNp63/BMP-7 signaling pathway modulates wound healing process through the regulation of matrilin-2.

p63 is a *p53* family member which encodes a nuclear transcription factor with pro-apoptotic potential [1]. Like p53 and p73 [2,3], p63 is expressed as multiple variants including TA (transactivating) and ΔN (non-transactivating) forms arising from alternative splicing (α, β, and γ) and alternative promoter usage, respectively [1]. ΔNp63 which lacks NH_2-terminal transactivation domain exhibits a dominant-negative activity against TAp63, TAp73, and wild-type p53 [1]. In contrast to *p53*, *p63* and *p73* are rarely mutated in primary human tumors [4]. Initial genetic analysis demonstrated that *p63*-deficient mice fail to generate spontaneous tumors [5,6]. Intriguingly, mice lacking *p63* die soon after birth due to severe dehydration with significant defects in limb, craniofacial and skin development, suggesting that p63 plays an important role in the regulation of epidermal development and morphogenesis.

Recent genetic studies revealed that TA or ΔN isoform alone does not complement epidermal defects in *p63*-deficient mice, indicating that both isoforms are required for proper epidermal development [7]. TAp63 is the earliest p63 isoform expressed during epidermal development [8]. On the other hand, ΔNp63 is predominantly expressed in basal layer and reduced in suprabasal keratinocytes [1,9]. Sommer et al. described that mice overexpressing ΔNp63 display profound wound healing defects [10]. In contrast to the previous viewpoint, several lines of evidence indicate that ΔNp63 transactivates certain subset of genes [11,12]. Considering that ΔNp63 possesses a transcriptional potential, it is of interest to identify ΔNp63-target(s) implicated in the regulation of wound healing process.

Matrilin-2 is composed of two von Willebrand factor A-like domains, multiple epidermal growth factor-like modules as well as COOH-terminal coiled-coil domain [13] and belonging to extracellular matrix matrilin superfamily including matrilin-1, -2, -3 and -4 [14]. Matrilin-1 and -3 are expressed largely in cartilage, whereas matrilin-2 and -4 are detectable in a wide variety of extracellular matrixes [15]. Matrilin-2 is only deposited at lower part of basement membrane or upper part of dermis next to basement membrane in human skin [16]. Recently, it has been shown that matrilin-2 is induced in response to muscle or liver injury [17,18].

In this study, we found that ΔNp63/BMP-7 signaling pathway is implicated in the modulation of wound healing process through transcriptional regulation of *matrilin-2* in human keratinocyte cells.

Materials and methods

Cell culture. HaCaT and SAOS-2 cells were grown in Dulbecco's modified Eagle's medium (DMEM) containing 10% heat-inactivated fetal bovine serum (FBS), 100 U/ml penicillin, and 100 μg/ml streptomycin. Cells were maintained at 37 °C in a water-saturated atmosphere of 95% air and 5% CO_2.

* Corresponding author. Address: Division of Biochemistry, Chiba Cancer Center Research Institute, 666-2 Nitona, Chuoh-ku, Chiba 260-8717, Japan. Fax: +81 43 265 4459.
E-mail address: akiranak@chiba-cc.jp (A. Nakagawara).

0006-291X/$ - see front matter © 2008 Elsevier Inc. All rights reserved.
doi:10.1016/j.bbrc.2008.02.128

Expression plasmid for BMP-7 and matrilin-2 luciferase reporters. Human *BMP-7* cDNA was amplified by PCR-based strategy. Sense and antisense primers used are as follows: 5′-CT**GGATCC**ACCGCCATGCACGTGCGCTCACTG-3′ (sense) and 5′-AA**GCGGCCGC**CTGTGGCAGCCACAGGCCCG-3′ (antisense). BamHI and NotI sites were shown in boldface type. PCR products were digested with BamHI and NotI and inserted into identical sites of pcDNA3-FLAG (Invitrogen) to give BMP-7-FLAG. The indicated luciferase reporters driven by *matrilin-2* promoter were generated using following primer sets: *MATN2*-promoter-1 (−289/+39), 5′-AT**ACGCGT**A AAGCTGCCTGTGTTCCG-3′ (sense) and 5′-AT**CTCGAG**TTGCTCCAAGTCCCATCC-3′ (antisense); *MATN2*-promoter-2 (−289/+205), 5′-AT**ACGCGT**AAAGCTGCCTGTGT TCCG-3′ (sense) and 5′-AT**CTCGAG**CTGCAGCCGCCGGCGCCT-3′ (antisense). MluI and XhoI sites were shown in boldface type. PCR products were then inserted into MluI and XhoI sites of pGL3-basic plasmid (Promega) upstream of *luciferase* gene. These constructs were verified by DNA sequencing (Applied Biosystems).

Transfection. Cells were transfected with the indicated expression plasmids using LipofectAMINE 2000 transfection reagent (Invitrogen) following the manufacturer's recommendations.

Short interference RNA. siRNA targeting human ΔNp63 was designed (5′-CAAUGCCCAGACUCAAUUU-3′) and purchased from Sigma. siRNA against human Smad4 (D-003902-05), human matrilin-2 (J-011329-09 and J-011329-11), luciferase (Luciferase GL2 Duplex) and control siRNA (siCONTROL) were purchased from Dharmacon. HaCaT cells were transfected with 25 nM of the indicated siRNAs using LipofectAMINE RNAiMAX (Invitrogen).

Luciferase reporter assay. HaCaT cells were transfected with 10 ng of pRL-TK *Renilla* luciferase cDNA (Promega) and 100 ng of matrilin-2 luciferase reporter or pGL3-basic plasmid and incubated with serum-free medium. Twenty-four hours after incubation, cells were treated with or without 100 ng/ml of human BMP-7. At the indicated time points after treatment, luciferase activities were determined by Dual-Luciferase Assay System (Promega) according to the manufacturer's recommendations.

Immunoblotting. Equal amounts of cell lysates were separated by 10% SDS–polyacrylamide gel electrophoresis (SDS–PAGE) and electrotransferred onto Immobilon-P Transfer Membrane (Millipore). Membranes were incubated with monoclonal anti-FLAG (M2, Sigma), monoclonal anti-Smad4 (B-8, Santa Cruz Biotechnology), monoclonal anti-p63 (4A4, NeoMarkers) or with polyclonal anti-actin (20–33, Sigma) followed by incubation with HRP-conjugated goat anti-mouse or with anti-rabbit IgG (Santa Cruz Biotechnology). Bound antibodies were detected by ECL system (Amersham Biosciences).

Reverse transcription PCR analysis. Total RNA was isolated from the indicated cells using the ISOGEN reagent (Nippon gene) according to the manufacturer's instructions and treated with RNase-free DNase I. Five micrograms of total RNA were used to synthesize first-strand cDNA using random primers and SuperScript II reverse transcriptase (Invitrogen). The list of primer sets used will be provided upon request.

Indirect Immunofluorescence staining. HaCaT cells were fixed in ice-cold acetone/methanol at room temperature for 1 min and then washed with ice-cold PBS. Cells were incubated with 4% normal goat serum (NGS) in PBS for 1 h at room temperature and then probed with monoclonal anti-p63 antibody followed by subsequent incubation with Alexa Fluor 488-conjugated goat anti-mouse IgG (Invitrogen). After extensive washing with PBS, cell nuclei were stained with 4,6-diamidino-2-phenylindole (DAPI).

In vitro wound healing. Subconfluent HaCaT cells were switched to serum-free medium and incubated for 24 h. Monolayer cultures of HaCaT cells were scratched by pipette tip and then incubated with 2% serum. Where indicated, HaCaT cells were exposed to mitomycin C (10 μg/ml) for 2 h [19].

Cell migration assays. Boyden chamber cell migration assay was performed using transwell chambers with 8-μm pore size membranes (Becton–Dickinson). HaCat cells were transfected with the indicated siRNAs. Twenty-four hours after transfection, medium was changed to fresh serum-free medium and subsequently incubated for 24 h. Cells were resuspended in serum-free medium and added to upper chamber at 1×10^5 cells/well and incubated for 24 h at 37 °C in a humidified atmosphere of 5% CO_2. Cells were stained with Calcein AM (BD Bioscieneces) for 20 min at room temperature followed by fixation in 3.7% formaldehyde for 10 min at room temperature. The migrated cells on lower surface of membrane were examined under a fluorescence microscopy.

Results

Expression of p63 at wound edge of human keratinocyte HaCaT cells

Since it has been unclear how p63 could regulate epidermal homeostasis, we examined expression levels of p63 in response to wounding. To this end, mechanical scratch was introduced on surface of confluent HaCaT cells. Cells were then transferred into fresh medium containing 2% FBS. At the indicated time periods after addition of FBS, cells were stained with anti-p63 antibody. As shown in Fig. 1A, p63 was undetectable in wound border 2 h after addition of FBS, whereas p63 levels returned to those in non-wounded cells 24 h after wounding.

Transcriptional regulation of matrinin-2 by ΔNp63

As described previously [17], matrilin-2 was transiently down-regulated in early phase of muscle injury and then increased in its late phase. Under our experimental conditions, p63 was undetectable in wound border in response to wounding. To address whether ΔNp63 could regulate *matrilin-2*, HaCaT cells were transfected with siRNA against luciferase (siLuc) or with ΔNp63 (siΔNp63). At the indicated time points after transfection, total RNA was subjected to RT-PCR. As shown in Fig. 1B, knockdown of ΔNp63 resulted in a significant reduction of *matrilin-2*, suggesting that *matrilin-2* is one of direct or indirect downstream targets of ΔNp63.

BMP-7 induces matrilin-2

During search of human *matrilinin-2*-promoter region, we found seven putative Smad-binding sites [20] (Fig. 2A). Since *BMP-7* is one of direct targets of p53 family including ΔNp63 [21], we examined whether BMP-7 could regulate *matrilin-2*. Consistent with recent observations [21], enforced expression of ΔNp63α resulted in a remarkable up-regulation of *BMP-7* but not of *BMP-2* and *BMP-4* (Fig. 2B). Similarly, knockdown of ΔNp63 reduced *BMP-7* but not *BMP-2* and *BMP-4* (Fig. 2C).

BMP-7 treatment induced *matrilin-2* in a time-dependent manner (Fig. 2D). BMP-7 had marginal effects on ΔNp63, whereas $p21^{WAF1}$ was significantly up-regulated in response to BMP-7 [22,23]. Our present findings suggest that BMP-7 induces *matrilin-2* through several Smad-binding sites.

BMP-7/Smad4 signaling pathway contributes to expression of matrilin-2

To further confirm a possible involvement of BMP-7 signaling pathway in the regulation of *matrilin-2*, knockdown of Smad4 was performed. As shown in Fig. 2E, siRNA against Smad4 efficiently reduced Smad4 in HaCaT cells. HaCaT cells were then transfected with siLuc or with siSmad4 and treated with BMP-7 or left untreated. Twenty-four hours after treatment, total RNA was analyzed for *matrilin-2* and $p21^{WAF1}$ by RT-PCR. As shown in Fig. 2F, BMP-7-mediated up-regulation of *matrilin-2* and $p21^{WAF1}$ was inhibited in Smad4-knockdown cells. As expected, knockdown of ΔNp63 led to a reduction of *matrilin-2* and *BMP-7*, whereas addition of BMP-7 partially attenuated inhibitory effects of siΔNp63 on *matrilin-2* (Fig. 2G).

Regulation of matrilin-2-promoter activity through ΔNp63/BMP-7 pathway

To examine effect of ΔNp63 and BMP-7 on promoter activity of *matrilin-2*, we generated luciferase reporters termed *MATN2*-promoter-1 (−289/+39) and *MATN2*-promoter-2 (−289/+205) (Fig. 3A). Twenty-four hours after starvation, HaCaT cells were transfected with *MATN2*-promoter-2 (−289/+205) and pRL-TK. Four hours after transfection, cells were treated with BMP-7 or left untreated. Consistent with our present results, luciferase activity driven by *MATN2*-promoter-2 (−289/+205) was significantly enhanced in response to BMP-7 as compared with those in untreated cells (Fig. 3B). Knockdown of ΔNp63 led to a significant reduction of luciferase activity driven by *MATN2*-promoter-2 (−289/+205) (Fig. 3C). Luciferase activity driven by *MATN2*-promoter-1 (−29/+39) was also decreased in ΔNp63-knocked down cells but to a

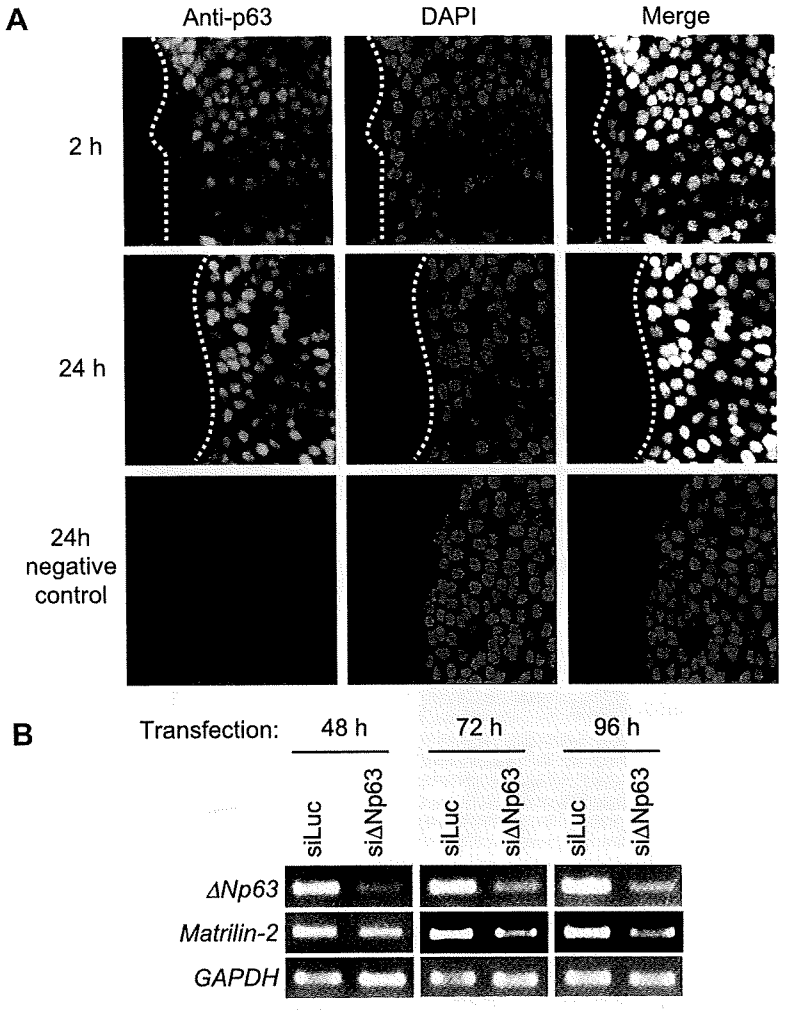

Fig. 1. Expression of p63 at wound edge and ΔNp63-dependent expression of *matrilin-2*. (A) Immunofluorescence staining. *In vitro* wound was introduced on surface of confluent HaCaT cells and cells were incubated with 2% FBS for the indicated time periods. Cells were then immunostained with anti-p63 antibody (left panels). Cell nuclei were stained with DAPI (middle panels). Merged images were shown in right panels. Negative control experiments were performed without primary antibody (bottom panels). White dots indicate positions of wound edge. (B) Effects of knockdown of ΔNp63 on *matrilin-2*. HaCaT cells were transfected with the indicated siRNAs. At the indicated time periods after transfection, total RNA was subjected to RT-PCR to examine expression levels of *ΔNp63* and *matrilin-2*. *GAPDH* was used as an internal control.

lesser degree, which might be due to its lower numbers of Smad-binding sites [22]. Furthermore, the decrease in the luciferase activity driven by *MATN2*-promoter-2 (−289/+205) in ΔNp63-knocking down cells was compensated by enforced expression of BMP-7 (Fig. 3D).

Migration of matrilin-2-knocked down cells in response to wounding

We evaluated quality of siRNAs against matrilin-2 (#9 and #11) by RT-PCR. As shown in Fig. 4A, both siRNAs efficiently knocked down *matrilin-2*. To ask whether ΔNp63 and/or matrilin-2 could be involved in the wound healing process, HaCaT cells were transfected with the indicated siRNAs and maintained without FBS. Twenty-four hours after starvation, wounds were made on surface of cells and cells were incubated with 2% FBS for 96 h. As shown in Fig. 4B, elimination of ΔNp63 promoted cell migration into wound as compared with control cells transfected with siLuc. Similarly, knocking down of matrilin-2 resulted in a remarkable induction of cell migration into wound (top panels of Fig. 4C). To rule out the possibility that introduction of wound might induce cell proliferation rather than cell migration, transfected HaCaT cells were exposed to mitomycin C to suppress cell proliferation [21]. Two hours after treatment with mitomycin C, mechanical scratch was made and cells were incubated with 2% FBS. As shown in middle and bottom panels of Fig. 4C, cell migration into wound was clearly observed 72 h after incubation with FBS, indicating that knockdown of ΔNp63 or matrilin-2 promotes cell migration in response to wounding.

To further confirm this issue, Boyden chamber assays were performed. Under our experimental conditions, transfected cells were allowed to migrate towards 2% FBS for 24 h. As seen in Fig. 4D, the increased number of ΔNp63- or matrilin-2-knockdown cells was detectable on lower side of membrane as compared with that of control cells transfected with siLuc.

Discussion

In this study, we found that matrilin-2 is one of downstream mediators of ΔNp63 and its expression is mediated through BMP-7/Smad signaling pathway. Consistent with recent observations [21], ΔNp63 transactivates *BMP-7*. Addition of purified BMP-7 resulted in a significant induction of *matrilin-2* in associa-

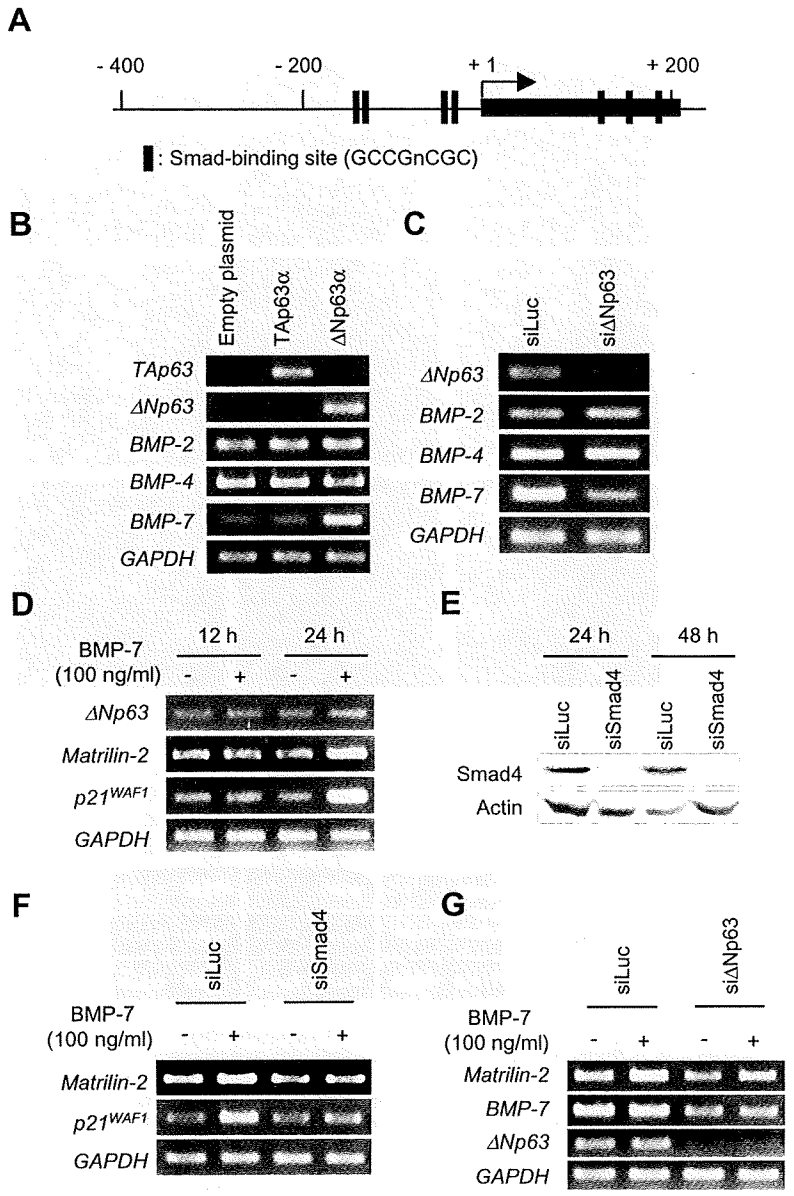

Fig. 2. BMP-7 induces *matrilin-2*. (A) Smad-binding sites in human *matrilin-2*-promoter region. Smad-binding sites are indicated by filled boxes. Numbers represent nucleotide positions relative to transcriptional initiation site (+1). (B) Enforced expression of ΔNp63 induces *BMP-7*. SAOS-2 cells were transfected with the indicated expression plasmids. Forty-eight hours after transfection, total RNA was subjected to RT-PCR to examine expression levels of *TAp63α*, *ΔNp63α* and *BMPs*. (C) Knockdown of ΔNp63 results in a reduction of *BMP-7*. HaCaT cells were transfected with siLuc or siΔNp63. Forty-eight hours after transfection, total RNA was subjected to RT-PCR. (D) Induction of *matrilin-2* in response to BMP-7. HaCaT cells were maintained without FBS for 24 h and then treated with human BMP-7 (100 ng/ml) or left untreated. At the indicated time points after treatment, total RNA was processed for RT-PCR to analyze *matrilin-2* expression. $p21^{WAF1}$ was used as a positive control. (E) Knockdown of Smad4. HaCaT cells were transfected with siLuc or siSmad4. At the indicated time periods after transfection, cell lysates were analyzed by immunoblotting using anti-Smad4 antibody. Actin was used as a loading control. (F) Knockdown of Smad4 inhibits BMP-7-mediated induction of *matrilin-2* and $p21^{WAF1}$. HaCaT cells were transfected with siLuc or siSmad4. Four hours after transfection, cells were transferred into fresh medium lacking FBS and incubated for 24 h. Cells were then treated with or without 100 ng/ml of BMP-7. Twenty-four hours after treatment, total RNA was subjected to RT-PCR. (G) BMP-7 attenuates inhibitory effect of siΔNp63 on *matrilin-2*. HaCaT cells transfected as in (C). Twenty-four hours after transfection, cells were exposed to BMP-7 (100 ng/ml). Twenty-four hours after treatment, *matrilin-2*, *BMP-7*, and *ΔNp63* expressions were examined by RT-PCR.

tion with phosphorylation of Smad1/5/8 (data not shown). Indeed, there exist seven putative Smad-binding sites within human *matrilin-2* promoter as well as exon 1 and knockdown of Smad4 inhibited BMP-7-dependent transactivation of *matrilin-2*. In contrast to the previous viewpoint, ΔNp63 has a transcriptional potential [11,12]. Koster et al. demonstrated that ΔNp63 is recruited onto p53/p63-responsive element [8]. Intriguingly, we found two putative p53/p63-responsive elements in 5′-upstream region of *matrilin-2* gene (data not shown) and knockdown of ΔNp63 led to a remarkable down-regulation of *matrilin-2*. Additionally, reduction of *matrilin-2*-promoter activity caused by siΔNp63 was recovered by BMP-7. Although it is unclear whether ΔNp63 could directly induce *matrilin-2*, it is likely that ΔNp63 promotes *matrilin-2* through BMP-7/Smad signaling pathway.

Another finding of our present study was that silencing of ΔNp63 or matrilin-2 results in a significant promotion of cell

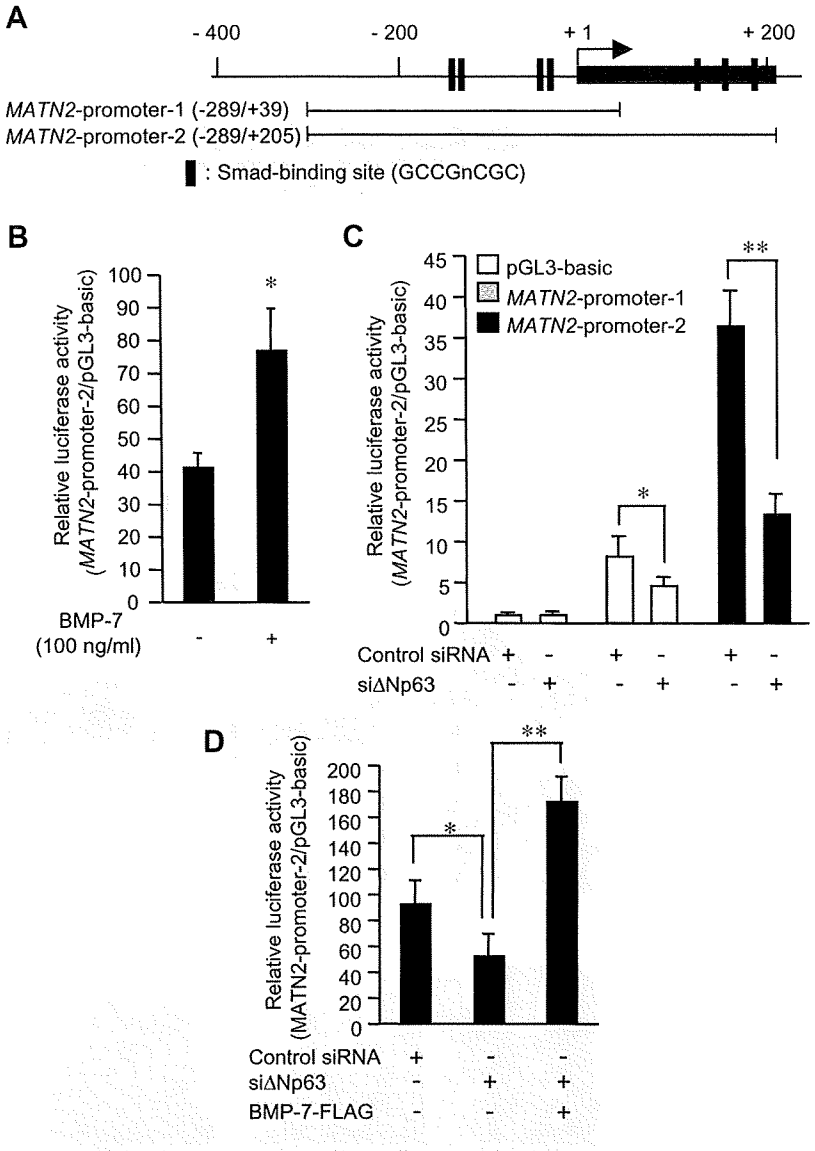

Fig. 3. Regulation of *matrilin-2*-promoter activity. (A) Schematic representations of *matrilin-2*-promoter region and *matrilin-2* luciferase reporters termed *MATN2*-promoter-1 (−289/+39) and *MATN2*-promoter-2 (−289/+205). Smad-binding sites are shown in solid boxes. (B) Induction of *matrilin-2*-promoter activity by BMP-7. HaCaT cells which were maintained without FBS for 24 h, were transfected with 10 ng of pRL-TK together with 100 ng of pGL3-basic plasmid or *MATN2*-promoter-2 (−289/+205). Four hours after transfection, cells were treated with or without 100 ng/ml of BMP-7 and incubated for 22 h. Cells were then lysed and both firefly and *Renilla* luciferase activities were measured. Firefly luminescence signal was normalized based on *Renilla* luminescence signal. Results were obtained at least four-independent experiments and represent as means ± SD $^{*}p < 0.01$. (C) Effect of knockdown ΔNp63 on *matrilin-2* reporter activity. Forty-eight hours after transfection with the indicated siRNAs, cells were transfected with 10 ng of pRL-TK together with 100 ng of pGL3-basic plasmid, *MATN2*-promoter-1 (−289/+39) or *MATN2*-promoter-2 (−289/+205) and luciferase activities were determined as in (B). $^{*}p < 0.05$; $^{**}p < 0.0001$. (D) BMP-7 attenuates inhibitory effect of siΔNp63 on *matrilin-2* reporter activity. HaCaT cells were transfected with control siRNA or with siΔNp63. Forty hours after transfection, cells were transfected with *MATN2*-promoter-2 (−289/+205) luciferase reporter and pRL-TK together with or without 100 ng of BMP-7-FLAG expression plasmid. Luciferase activities were measured at 40 h post-transfection. $^{*}p < 0.05$; $^{**}p < 0.01$.

migration into wound without cell proliferation. Our present observations were consistent with recent results showing that lack of ΔNp63 expression correlates with the highest levels of cell migration [24]. Additionally, transgenic mice over-expressing ΔNp63 in skin exhibit massive wound healing defects and decreased skin thickness [10]. ΔNp63 is transiently repressed in response to wounding and then ΔNp63 is expressed at basal levels [25], suggesting that proper temporal expression of ΔNp63 is required for normal wound healing process.

As described [16], matrilin-2 is expressed in several human tissues and associated with basement membrane of muscle and various epithelia. Additionally, matrilin-2 interacts with extracellular matrix proteins such as collagens, proteoglycans and laminins, indicating that matrilin-2 acts as an adaptor protein in extracellular matrix and might play an important role in matrix assembly. During wound healing process, cell migration into wound takes places and then extracellular matrix is newly generated. Prior to cell migration in response to wounding, extracellular matrix around wound border should be degraded to facilitate cell migration into wound. Thus, it is likely that transient down-regulation of ΔNp63 and matrilin-2 in response to wounding might be an early step for wound healing process.

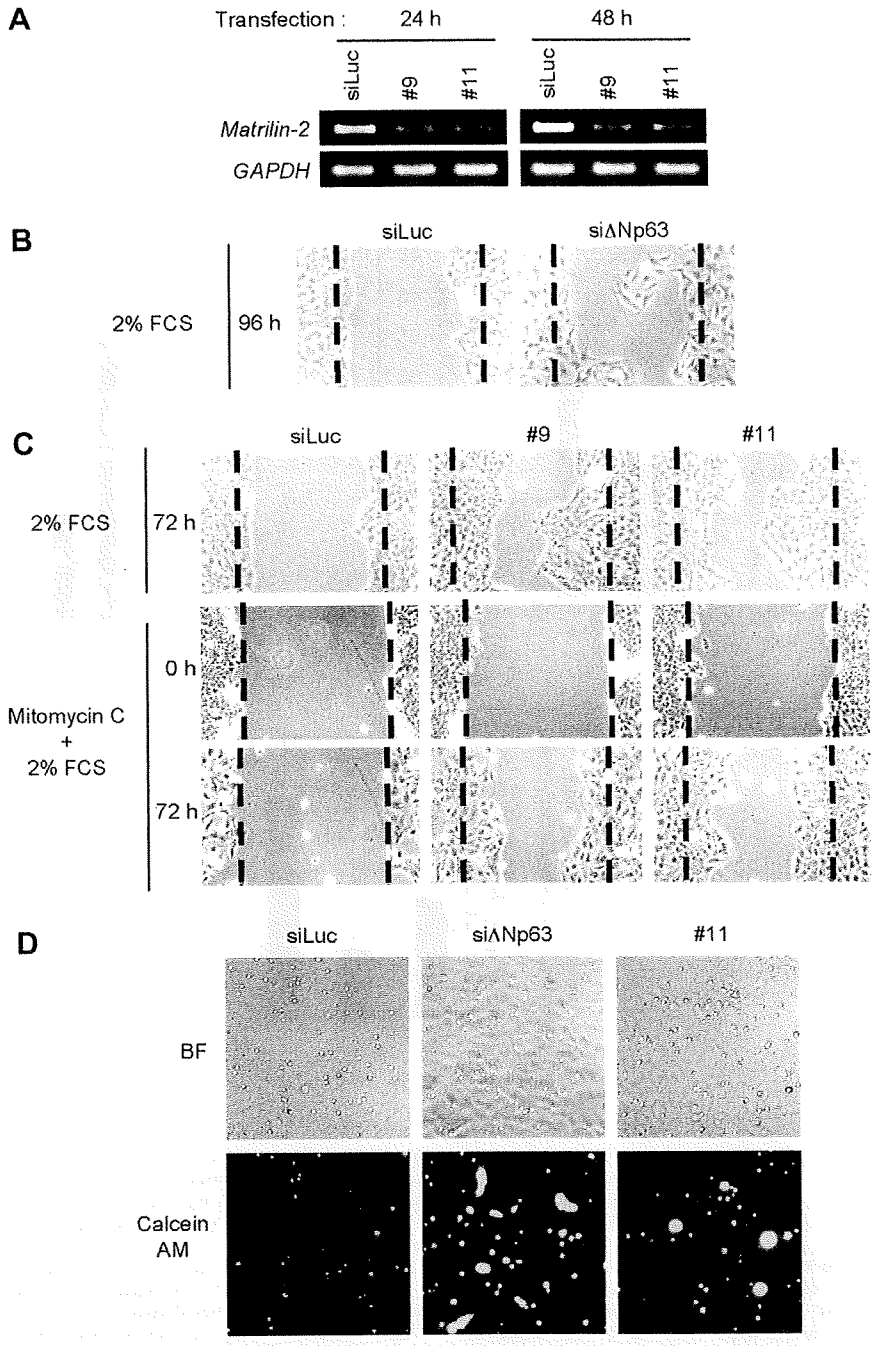

Fig. 4. *In vitro* wound healing assay. (A) Knockdown of *matrilin-2*. HaCaT cells were transfected with the indicated matrilin-2 siRNAs (#9 and #11). At the indicated time points after transfection, *matrilin-2* expression was examined by RT-PCR. (B,C) Scratch wound assay. Confluent HaCaT cells transfected with the indicated siRNAs were incubated with FBS-free medium for 24 h. FBS-deprived cells were scratched and medium was changed into fresh medium containing 2% of FBS. Wound edges were photographed 96 h after FBS addition. Dotted lines indicate positions of wound edge 0 h after FBS addition (B). HaCaT cells transfected with the indicated siRNAs were treated with 10 μg/ml of mitomycin C for 2 h before FBS deprivation. After FBS deprivation, wounds were introduced and cells were cultured in fresh medium containing 2% FBS. Wound edges were photographed 0 and 72 h after FBS addition. (D) Migration assay. HaCaT cells were transfected with the indicated siRNAs. Twenty-four hours after transfection, medium was changed into fresh FBS-free medium. Twenty-four after incubation, 10^5 cells were seeded into Boyden chamber and incubated for 24 h. Cells observed on lower side of membrane were stained with Calcein AM and migrating cells were detected by fluorescence microscopy. Total pore number in the same area was photographed by bright-field microscopy (BF).

Acknowledgments

This work was supported in part by a Grant-in-Aid from the Ministry of Health, Labour and Welfare for Third Term Comprehensive Control Research for Cancer, a Grant-in-Aid for Scientific Research on Priority Areas from the Ministry of Education, Culture, Sports, Science and Technology, Japan, a Grant-in-Aid for Scientific Research from Japan Society for the Promotion of Science, Uehara Memorial Foundation and Hisamitsu Pharmaceutical Co.

References

[1] A. Yang, M. Kaghad, Y. Wang, E. Gillett, M.D. Fleming, V. Dotsch, N.C. Andrews, D. Caput, F. McKeon, p63, a p53 homolog at 3q27–29, encodes multiple products with transactivating, death-inducing, and dominant-negative activities, Mol. Cell 2 (1998) 305–316.

[2] M. Kaghad, H. Bonnet, A. Yang, L. Creancier, J.C. Biscan, A. Valent, A. Minty, P. Chalon, J.M. Lelias, X. Dumont, P. Ferrara, F. McKeon, D. Caput, Monoallelically expressed gene related to p53 at 1p36, a region frequently deleted in neuroblastoma and other human cancers, Cell 90 (1997) 809–819.

[3] J.C. Bourdon, K. Fernandes, F. Murray-Zmijewski, G. Liu, A. Diot, D.P. Xirodimas, M.K. Saville, D.P. Lane, p53 isoforms can regulate p53 transcriptional activity, Genes Dev. 19 (2005) 2122–2137.

[4] S. Ikawa, A. Nakagawara, Y. Ikawa, p53 family genes: structural comparison, expression and mutation, Cell Death Differ. 6 (1999) 1154–1161.

[5] A. Yang, R. Schweitzer, D. Sun, M. Kaghad, N. Walker, R.T. Bronson, C. Tabin, A. Sharpe, D. Caput, C. Crum, F. McKeon, p63 is essential for regenerative proliferation in limb, craniofacial and epithelial development, Nature 398 (1999) 714–718.

[6] A.A. Mills, B. Zheng, X.J. Wang, H. Vogel, D.R. Roop, A. Bradley, p63 is a p53 homologue required for limb and epidermal morphogenesis, Nature 398 (1999) 708–713.

[7] E. Candi, A. Rufini, A. Terrinoni, D. Dinsdale, M. Ranalli, A. Paradisi, V. De Laurenzi, L.G. Spagnoli, M.V. Catani, S. Ramadan, R.A. Knight, G. Melino, Differential roles of p63 isoforms in epidermal development: selective genetic complementation in p63 null mice, Cell Death Differ. 13 (2006) 1037–1047.

[8] M.I. Koster, D. Dai, D.R. Roop, Conflicting roles for p63 in skin development and carcinogenesis, Cell Cycle 6 (2007) 269–273.

[9] R. Parsa, A. Yang, F. McKeon, H. Green, Association of p63 with proliferative potential in normal and neoplastic human keratinocytes, J. Invest. Dermatol. 113 (1999) 1099–1105.

[10] M. Sommer, N. Poliak, S. Upadhyay, E. Ratovitski, B.D. Nelkin, L.A. Donehower, D. Sidransky, DeltaNp63alpha overexpression induces downregulation of Sirt1 and an accelerated aging phenotype in the mouse, Cell Cycle 5 (2006) 2005–2011.

[11] G. Wu, M. Osada, Z. Guo, A. Fomenkov, S. Begum, M. Zhao, S. Upadhyay, M. Xing, F. Wu, C. Moon, W.H. Weastra, W.M. Koch, R. Mantovani, J.A. Califano, E. Ratovitski, D. Sidransky, B. Trink, ΔNp63α up-regulates the *Hsp70* gene in human cancer, Cancer Res. 65 (2005) 758–766.

[12] C. Beretta, A. Chiarelli, B. Testoni, R. Mantovani, L. Guerrini, Regulation of the cyclin-dependent kinase inhibitor $p57^{Kip2}$ expression by p63, Cell Cycle 4 (2005) 1625–1631.

[13] F. Deak, D. Piecha, C. Bachrati, M. Paulsson, I. Kiss, Primary structure and expression of matrilin-2, the closest relative of cartilage matrix protein within the von Willebrand factor type A-like module superfamily, J. Biol. Chem. 272 (2007) 9268–9274.

[14] R. Wagener, H.W. Ehlen, Y.P. Ko, B. Kobbe, H.H. Mann, G. Sengle, M. Paulsson, The matrilins-adaptor proteins in the extracellular matrix, FEBS Lett. 579 (2005) 3323–3329.

[15] F. Deak, R. Wagener, I. Kiss, M. Paulsson, The matrilins: a novel family of oligomeric extracellular matrix proteins, Matrix Biol. 18 (1999) 55–64.

[16] D. Piecha, C. Wiberg, M. Morgelin, D.P. Reinhardt, F. Deak, P. Maurer, M. Paulsson, Matrilin-2 interacts with itself and with other extracellular matrix proteins, Biochem. J. 367 (2002) 715–721.

[17] S.C. Goetsch, T.J. Hawke, T.D. Gallarde, J.A. Richardson, D.J. Garry, Transcriptional profiling and regulation of the extracellular matrix during muscle regeneration, Physiol. Genomics 14 (2003) 261–271.

[18] E. Szabo, C. Lodi, E. Korpos, E. Batmunkh, Z. Rottenberger, F. Deak, I. Kiss, A.M. Tokes, G. Lotz, V. Laszlo, A. Kiss, Z. Schaff, P. Nagy, Expression of matrilin-2 in oval cells during rat liver regeneration, Matrix Biol. 26 (2007) 554–560.

[19] L.G. Hudson, L.J. McCawley, Contributions of the epidermal growth factor receptor to keratinocyte motility, Microsc. Res. Tech. 43 (1998) 444–455.

[20] K. Kusanagi, H. Inoue, Y. Ishidou, H.K. Mishima, M. Kawabata, K. Miyazono, Characterization of a bone morphogenetic protein-responsive Smad binding element, Mol. Biol. Cell 11 (2000) 555–565.

[21] W. Yan, X. Chen, Targeted repression of bone morphogenetic protein 7, a novel target of the p53 family, triggers proliferative defect in p53-deficient breast cancer cells, Cancer Res. 67 (2007) 9117–9124.

[22] A. Franzen, N.E. Heldin, BMP-7-induced cell cycle arrest of anaplastic thyroid carcinoma cells via p21(CIP1) and p27(KIP1), Biochem. Biophys. Res. Commun. 285 (2001) 773–781.

[23] K. Pardali, M. Kowanetz, C.H. Heldin, A. Moustakas, Smad pathway-specific transcriptional regulation of the cell cycle inhibitor $p21^{WAF1/Cip1}$, J. Cell Physiol. 204 (2005) 260–272.

[24] C.E. Barbieri, L.J. Tang, K.A. Brown, J.A. Pietenpol, Loss of p63 leads to increased cell migration and up-regulation of genes involved in invasion and metastasis, Cancer Res. 66 (2006) 7589–7597.

[25] C. Bamberger, A. Hafner, H. Schwale, S. Werner, Expression of different p63 variants in healing skin wounds suggests a role of p63 in reepithelialization and muscle repair, Wound Repair Regen. 13 (2005) 41–50.

Biochemical and Biophysical Research Communications 370 (2008) 594–598

Contents lists available at ScienceDirect

Biochemical and Biophysical Research Communications

journal homepage: www.elsevier.com/locate/ybbrc

A newly identified dependence receptor UNC5H4 is induced during DNA damage-mediated apoptosis and transcriptional target of tumor suppressor p53

Hong Wang [a,b], Toshinori Ozaki [a,c], M. Shamim Hossain [a,c], Yohko Nakamura [a], Takehiko Kamijo [a], Xindong Xue [b], Akira Nakagawara [a,c,*]

[a] Division of Biochemistry, Chiba Cancer Center Research Institute, 666-2 Nitona, Chuoh-ku, Chiba 260-8717, Japan
[b] Department of Pediatric, Shengjing Hospital of China Medical University, Shenyang 110004, China
[c] Department of Molecular Biology and Oncology, Chiba University Graduate School of Medicine, Chiba 260-8717, Japan

ARTICLE INFO

Article history:
Received 26 March 2008
Available online 8 April 2008

Keywords:
Adriamycin
Apoptosis
DNA damage
p53
Transcription
UNC5H4

ABSTRACT

UNC5H4 is a netrin-1 receptor UNC5H family member. In this study, we found that *UNC5H4* is a direct transcriptional target of p53. During adriamycin (ADR)-mediated apoptosis, *UNC5H4* was significantly induced in *p53*-proficient U2OS cells but not in *p53*-deficient H1299 cells. Enforced expression of p53 induced *UNC5H4*. Consistent with these results, siRNA-mediated knockdown of p53 in U2OS cells attenuated ADR-dependent induction of *UNC5H4*. Indeed, we found four putative p53-responsive elements within intron 1 of *UNC5H4* gene. Luciferase reporter assay and ChIP analysis demonstrated that, among them, two tandem elements respond to exogenous p53 which is efficiently recruited onto them. Furthermore, enforced expression of UNC5H4 remarkably reduced number of drug-resistant colonies in *p53*-proficient cells but not in *p53*-deficient cells, suggesting that UNC5H4-induced apoptosis is dependent on *p53* status. siRNA-mediated knockdown of UNC5H4 rendered U2OS cells resistant to ADR. Collectively, our present results suggest that UNC5H4 amplifies p53-dependent apoptotic response.

Type I transmembrane receptors such as DCC (deleted in colorectal cancer) and UNC5H have been considered to belong to the so-called dependence receptor family [1,2]. These receptors share functional similarity to promote apoptosis without their respective ligands including netrin family, but inhibit apoptosis when bound to these ligands [3]. As described [1], DCC was one of caspase substrates and served as a caspase amplifier under conditions in which the ligand is unavailable. Extensive studies suggested that DCC acts as a tumor suppressor [4], however, *DCC* is rarely mutated in human cancers [5]. Mammalian UNC5H family is composed of UNC5H1–4 [6–8]. Among them, UNC5H4 has been recently found in human genome database [9]. Thiebault et al. described that expression levels of *UNC5H1–3* are strongly down-regulated in various primary tumors which is associated with loss of heterozygosity (LOH) within *UNC5H* loci and enforced expression of UNC5H1, UNC5H2 or UNC5H3 inhibits malignant transformation, which is related to their pro-apoptotic activity [10]. According to their results, UNC5H-mediated apoptosis was dependent on their cytoplasmic death domain and potent caspase inhibitor abrogated their pro-apoptotic activity. Consistent with these observations, UNC5H1–3 contained classic caspase cleavage site (DXXD) [11] and caspase-mediated cleavage of UNC5H was required for cell death induction [2]. Although UNC5H family has pro-apoptotic activity [12], the precise molecular mechanisms behind UNC5H-mediated apoptosis remained unclear.

Of note, *UNC5H2* is a direct transcriptional target of p53 and UNC5H2-mediated apoptosis is regulated in a p53-dependent manner [13]. Based on their results, netrin-1 inhibited p53-dependent apoptosis without affecting expression levels of p53. Alternatively, Llambi et al. found that UNC5H2 interacts with death-associated protein kinase (DAP-kinase) and their interaction enhances catalytic activity of DAP-kinase [14]. Intriguingly, DAP-kinase required functional p53 for induction of apoptosis [15]. In contrast to UNC5H1–3, little is known about functional significance of UNC5H4. In the present study, we found that *UNC5H4* is a direct transcriptional target of p53 and UNC5H4-mediated apoptosis is dependent on *p53* status.

Materials and methods

Cell lines and culture. Human osteosarcoma U2OS and SAOS-2 cells were maintained in Dulbecco's modified Eagle's medium (DMEM) supplemented with 10% heat-inactivated fetal bovine serum (FBS, Invitrogen), penicillin (50 U/ml) and streptomycin (50 μg/ml). Human lung carcinoma H1299 cells were cultured in RPMI 1640 medium supplemented with 10% heat-inactivated FBS and antibiotic mixture. Cells were grown at 37 °C in a humidified atmosphere of 5% CO_2 in the air. Where indicated, cells were exposed to adriamycin (ADR) at a final concentration of 1 μM.

* Corresponding author. Address: Division of Biochemistry, Chiba Cancer Center Research Institute, 666-2 Nitona, Chuoh-ku, Chiba 260-8717, Japan. Fax: +81 43 265 4459.
E-mail address: akiranak@chiba-cc.jp (A. Nakagawara).

0006-291X/$ - see front matter © 2008 Elsevier Inc. All rights reserved.
doi:10.1016/j.bbrc.2008.03.152

Transfection. Cells were transfected with the indicated expression plasmids using LipofectAMINE 2000 transfection reagent (Invitrogen) according to the manufacturer's instructions.

Cell survival assay. Cells were seeded at a density of 5×10^3 cells/96-well cell culture plates and allowed to attach overnight. Cells were then treated with 1 μM of ADR. At the indicated time points after ADR treatment, 10 μl of a modified 3-(4,5-dimethylthiazol-2-yl) 2,5-diphenyl-tetrazolium bromide solution (Dojindo) were added to the culture and reaction mixtures were incubated at 37 °C for 1 h. The absorbance readings for each well were carried out at 570 nm using the microplate reader (Model 450, Bio-Rad Laboratories).

RT-PCR. Total RNA was isolated from the indicated cells by using RNeasy Mini Kit (Qiagen) according to the manufacturer's recommendations and reverse transcribed in the presence of random primers and SuperScript II reverse transcriptase (Invitrogen). The resultant first-strand cDNA was amplified by PCR to measure expression levels of genes of interest. The oligonucleotide primers used in this study were as follows: *p53*, 5′-ATTTGATGCTGTCCCCGGACGATATTGAAC-3′ (sense) and 5′-ACCCTTTTTGGACTTCAGGTGGCTGGAGTG-3′ (antisense); *p21*^{WAF1}, 5′-ATGAAATT CACCCCCTTTCC-3′ (sense) and 5′-CCCTAGGCTGTGCTCACTTC-3′ (antisense); *Bax*, 5′-TTTGCTTCAGGGTTTCATCC-3′ (sense) and 5′-CAGTTGAAGTTGCCGTCAGA-3′ (antisense); *UNC5H4*, 5′-TGAACTGCAGATGCCATAGG-3′ (sense) and 5′-GGTTTCAGG GACACTGTGGT-3′ (antisense); *GAPDH*, 5′-ACCTGACCTGCCGTCTAGAA-3′ (sense) and 5′-TCCACCACCCTGTTGCTGTA-3′ (antisense). PCR products were separated by 1.5% agarose gel electrophoresis and visualized by ethidium bromide staining.

Immunoblotting. Cells were washed in ice-cold phosphate-buffered saline (PBS) and lysed in SDS-sample buffer containing 10% glycerol, 5% β-mercaptoethanol, 2.3% SDS and 62.5 mM Tris–HCl (pH 6.8). The protein concentration of cell lysates was determined by using Bio-Rad protein assay dye reagent (Bio-Rad Laboratories) according to the manufacturer's instructions. Bovine serum albumin (BSA) was used as a standard. Equal amounts of cell lysates were separated by 10% SDS–polyacrylamide gel electrophoresis, electro-transferred onto Immobilon-P membrane filters (Millipore) and blocked with 0.3% non-fat milk in Tris-buffered saline (TBS) containing 0.1% Tween 20 at 4 °C. The membranes were probed with monoclonal anti-p53 (DO-1: Oncogene Research Products), polyclonal anti-phospho-p53 at Ser-15 (Cell Signaling Technology), polyclonal anti-p21^{WAF1} (H-164, Santa Cruz Biotechnology), polyclonal anti-PARP (Cell Signaling Technology) or with anti-actin (20-33: Sigma) antibody at room temperature for 1 h followed by incubation with horseradish peroxidase-conjugated secondary antibodies (Cell Signaling Technology) at room temperature for 1 h. Immunoreactive bands were visualized by using ECL system (Amersham Biosciences) according to the manufacturer's instructions.

Establishment of p53-knocked down cell clones. U2OS cells were transfected with the empty plasmid (pSUPER, OligoEngine) or with the expression plasmid for siRNA against p53 (pSUPER-p53). Forty-eight hours after transfection, cells were transferred into the fresh medium containing G418 (Sigma) at a final concentration of 500 μg/ml and incubated for two weeks. Then, G418-resistant clones were picked up and cultured in the presence of G418. Expression levels of p53 in each cell clone were analyzed by immunoblotting.

Construction of luciferase reporter plasmids. The indicated luciferase reporter constructs driven by putative p53-responsive elements of *UNC5H4* gene were generated by using the following primer sets: RE1, 5′-GAGCTCATGTTGGCCAGGCTAGTC-3′ (sense) and 5′-GTGCTCACAGGGCAATGACTCACCTC-3′ (antisense); RE2, 5′-GGTACCT CATCCTCTGAACGTTAAC-3′ (sense) and 5′-GGTACCTAAAGGGACTAGATCATG-3′ (antisense); RE3, 5′-GAGCTCTCAGATTGCATGTCTGTAC-3′ (sense) and 5′-GAGCTCAGC CTCACATAACACAGAGT-3′ (antisense); RE4, 5′-GAGCTCTAGGGCAGTTAATCTTGC-3′ (sense) and 5′-GAGCTCACCTATGAAATGGTGGAG-3′ (antisense). The resultant PCR products were gel-purified and inserted into appropriate restriction sites of pGL3-promoter plasmid (Promega) to give p53-RE1, p53-RE2, p53-RE3 and p53-RE4. The constructs were verified by DNA sequencing (Applied Biosystems).

Luciferase reporter assay. *p53*-deficient H1299 cells were seeded at a density of 5×10^4 cells/12-well cell culture plates and allowed to attach overnight. Cells were transiently co-transfected with 100 ng of pGL3-promoter plasmid (Promega), p53-RE1, p53-RE2, p53-RE3 or p53-RE4, 10 ng of *Renilla* luciferase reporter construct (pRL-TK, Promega) and 25 ng of the expression plasmid for FLAG-p53. Total amount of plasmid DNA per transfection was kept constant (510 ng) with pcDNA3. Forty-eight hours after transfection, cells were lysed and their luciferase activities were measured by using Dual-Luciferase Assay System (Promega) according to the manufacturer's instructions. The firefly luminescence signal was normalized based on the *Renilla* luminescence signal.

Chromatin immunoprecipitation (ChIP) assay. ChIP assay was performed as described [16]. In brief, H1299 cells were transfected with the empty plasmid or with the expression plasmid for p53. Forty-eight hours after transfection, cells were cross-linked with 1% formaldehyde in medium for 10 min at 37 °C. Cross-linked chromatin was prepared from cells and sonicated to an average length of 200–800 nucleotides, precleaned with salmon sperm DNA/protein A-agarose beads and immunoprecipitated with normal mouse serum (NMS) or with monoclonal anti-p53 antibody. The immunoprecipitates were eluted with 100 μl of elution buffer (1% SDS and 1 mM $NaHCO_3$). Formaldehyde-mediated cross-links were reversed by heating at 65 °C for 4 h and the reaction mixtures were treated with proteinase K at 45 °C for 1 h. Genomic DNA was purified using the QIAquick PCR purification kit (Qiagen). Purified DNA was amplified by PCR using the following primer sets: RE1, 5′-GAGCTCATGTTGGCCAGGCTAGTC-3′ (sense) and 5′-GTGCTCACAGGGCAATGACT CACCTC-3′ (antisense); RE2, 5′-GGTACCTCATCCTCTGAACGTTAAC-3′ (sense) and 5′-GGTACCTAAAGGGACTAGATCATG-3′ (antisense); RE3, 5′-TCAGATTGCATGTCTG TAC-3′ (sense) and 5′-AGCCTCACATAACACAGAGT-3′ (antisense).

Colony formation assay. U2OS and H1299 cells were transfected with the empty plasmid (pcDNA3) or with the expression plasmid encoding UNC5H4. Forty-eight hours after transfection, cells were transferred into fresh medium supplemented with G418 (400 μg/ml). After two weeks of selection, drug-resistant colonies were stained with Giemsa's solution and number of drug-resistant colonies was scored.

siRNA-mediated knockdown of UNC5H4. SAOS-2 cells were transfected with 10 nM of control siRNA or with siRNA against UNC5H4 (Dharmacon) by using LipofectAMINE RNAiMAX (Invitrogen) according to the manufacturer's recommendations. A list of siRNA sequences used will be provided upon request. Forty-eight hours after transfection, total RNA was prepared and analyzed for expression levels of *UNC5H4* by RT-PCR.

Flow cytometry. Forty-eight hours after the treatment with ADR (1 μM), floating and attached cells were collected, washed in ice-cold PBS and fixed in 70% ethanol at −20 °C. The cells were washed in ice-cold PBS and resuspended in phosphate-citrate buffer (4 mM citric acid and 200 mM Na_2HPO_4) and kept at room temperature for 15 min. Nuclear DNA was stained with propidium iodide (40 μg/ml) in the presence of RNase A (10 μg/ml) and the reaction mixture was incubated in the dark for 30 min. After the incubation with propidium iodide, DNA content of cells was examined by FACScan flow cytometer (Beckton Dickinson) using CellQuest software.

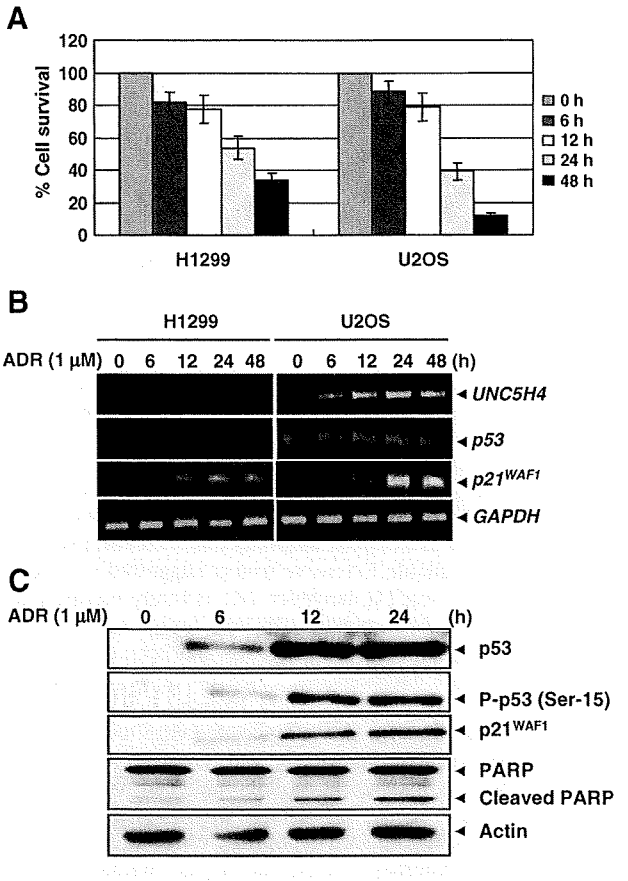

Fig. 1. Transcriptional activation of *UNC5H4* in *p53*-proficient cells but not in *p53*-deficient cells exposed to DNA damage. (A) Cell survival assays. *p53*-deficient H1299 cells and *p53*-proficient U2OS cells were treated with 1 μM of ADR. At the indicated time points, cell viability was examined by MTT assay. (B) RT-PCR. At the indicated time points after ADR treatment (1 μM), total RNA was prepared from H1299 (left panels) and U2OS (right panels) cells and analyzed for expression levels of *UNC5H4*, *p53* and *p21*^{WAF1}. Amplification of *GAPDH* was used as an internal control. (C) Immunoblotting. U2OS cells were exposed to ADR (1 μM). At the indicated time points, cell lysates were prepared and subjected to immunoblotting with the indicated antibodies. Immunoblotting for actin is shown as a loading control.

Results

DNA damage-induced up-regulation of UNC5H4

To examine expression patterns of *UNC5H4* and *p53*-related genes in response to DNA damage, *p53*-deficient lung carcinoma H1299 and *p53*-proficient osteosarcoma U2OS cells were exposed to 1 μM of adriamycin (ADR). Both cells underwent apoptosis as examined by MTT assay (Fig. 1A). Similar results were also obtained by FACS analysis (data not shown). During ADR-mediated apoptosis, $p21^{WAF1}$ which is one of p53-target genes [17] and *UNC5H4* were strongly induced in U2OS cells (Fig. 2B). Similar results were also obtained in neuroblastoma SH-SY5Y cells bearing wild-type *p53* (data not shown). In contrast, *UNC5H4* was undetectable in H1299 cells exposed to ADR, however, ADR-mediated up-regulation of $p21^{WAF1}$ was detectable, which might be due to the induction of another p53 family member p73 (data not shown). Immunoblot analysis revealed that ADR treatment results in a remarkable accumulation of p53, phospho-p53 at Ser-15, cleaved PARP and $p21^{WAF1}$ in U2OS cells (Fig. 1C).

UNC5H4 is a transcriptional target of p53

These observations prompted us to examine whether *UNC5H4* could be a transcriptional target of p53. To address this issue, H1299 cells were transfected with the expression plasmid encoding p53. Time course experiments demonstrated that p53 induces expressions of *UNC5H4*, $p21^{WAF1}$ and *Bax* [18] in a time-dependent manner (Fig. 2A). Transfection with the empty plasmid alone had undetectable effect on *UNC5H4* (data not shown). To further confirm this notion, we established two stable U2OS transfectants in which p53 was knocked down (N-1 and N-2) and one control transfectant (C-1). These transfectants were then treated with ADR and analyzed for expression levels of *UNC5H4*. As seen in Fig. 2B, p53 was successfully knocked down and ADR-mediated induction of p53 and $p21^{WAF1}$ were undetectable in N-1 and N-2 cell clones. ADR-mediated up-regulation of p53 and $p21^{WAF1}$ were observed in C-1 cell clone. ADR treatment significantly induced expression of *UNC5H4* in C-1 cell clone, whereas exposure to ADR had undetectable effect on *UNC5H4* in N-1 and N-2 cell clones, suggesting that *UNC5H4* is a transcriptional target of p53 and also involved in DNA damage response.

p53 enhances the promoter activity of UNC5H4 gene

It has been shown that *UNC5H2* composed of 17 exons is mapped at chromosome 10 and two functional p53-binding sequences are detectable within intron 1 of *UNC5H2* [13]. During extensive search for putative p53-responsive element(s) within intron 1 of *UNC5H4* gene, we identified four candidate p53-responsive elements (p53-RE1-4). To verify whether these elements could respond to p53, each of these elements was subcloned upstream of pGL3-promoter plasmid and luciferase reporter assays

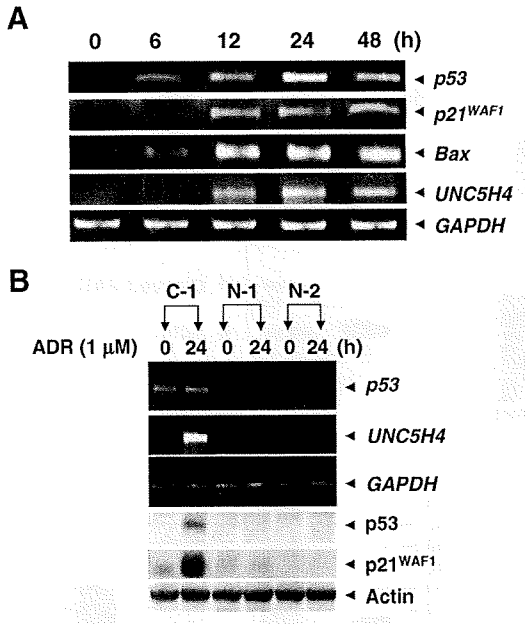

Fig. 2. p53-mediated transcriptional activation of *UNC5H4*. (A) Time course experiments. H1299 cells were transfected with the expression plasmid encoding p53. At the indicated time points, total RNA was prepared and analyzed for expression levels of *p53*, $p21^{WAF1}$, *Bax* and *UNC5H4* by RT-PCR. (B) siRNA-mediated knockdown of p53 attenuates ADR-dependent up-regulation of *UNC5H4*. U2OS cells were transfected with the empty plasmid or with the expression plasmid for siRNA against p53. Forty-eight hours after transfection, cells were transferred into fresh medium containing G418 (500 μg/ml) and maintained for two weeks. We then established control (C-1) and knockdown transfectants (N-1 and N-2). These stable transfectants were treated with 1 μM of ADR. Twenty-four hours after the exposure to ADR, total RNA and cell lysates were prepared and subjected to RT-PCR (upper panels) and immunoblotting (lower panels), respectively.

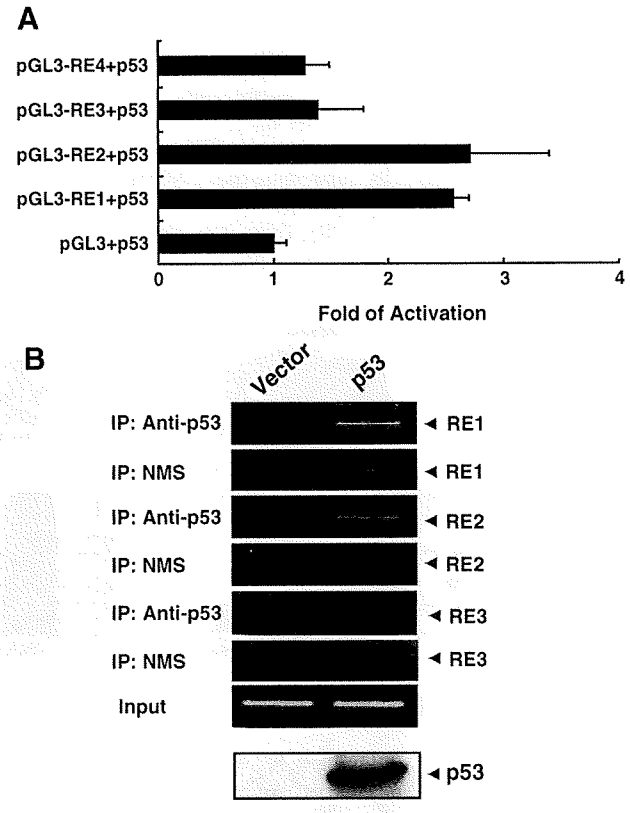

Fig. 3. *UNC5H4* is a direct target of p53. (A) Luciferase reporter assay. H1299 cells were co-transfected with 100 ng of the indicated luciferase reporter plasmids, 10 ng of *Renilla* luciferase reporter and 25 ng of expression plasmid for p53. Total amount of plasmid DNA per each transfection was kept constant (510 ng) with pcDNA3. All transfections were carried out in triplicate. Forty-eight hours after transfection, cells were lysed and their luciferase activities were measured by Dual-Luciferase Assay System. The firefly luciferase activity was normalized based on *Renilla* luciferase activity. Graphs indicate the average of three independent experiments. (B) ChIP assay. Cross-linked chromatin was prepared from H1299 cells transfected with the empty plasmid or with the expression plasmid for p53, sonicated to an average length of 200–800 nucleotides and immunoprecipitated with normal mouse serum (NMS) or with monoclonal anti-p53 antibody. Precipitated genomic DNA was amplified by PCR using the indicated primer sets (upper panels). Lower panel shows the expression of exogenous p53 as examined by immunoblotting.

were performed. As shown in Fig. 3A, luciferase activity driven by p53-RE1 or p53-RE2 was significantly enhanced by co-expression with p53, whereas p53 had marginal effects on p53-RE3 and p53-RE4. To determine whether p53 could be recruited onto p53-RE1 and/or p53-RE2, we performed chromatin immunoprecipitation (ChIP) assays. H1299 cells were transfected with the empty plasmid or with the expression plasmid for p53. Forty-eight hours after transfection, cross-linked chromatin was immunoprecipitated with normal mouse serum (NMS) or with monoclonal antibody against p53 and subjected to PCR-based amplification. As shown in Fig. 3B, genomic fragment containing p53-RE1 or p53-RE2 was precipitated with anti-p53 antibody, suggesting that p53 is recruited onto p53-RE1 and p53-RE2 in cells. On the other hand, genomic fragment including p53-RE3 was not precipitated with anti-p53 antibody. Similarly, p53 was not recruited onto p53-RE4 (data not shown).

UNC5H4-mediated apoptosis is dependent on p53 status

We next examined whether UNC5H4 could induce apoptosis. *p53*-proficient U2OS and *p53*-deficient H1299 cells were transfected with the empty plasmid or with the expression plasmid for UNC5H4. Forty-eight hours after transfection, cells were maintained in fresh medium containing G418. After two weeks of selection, drug-resistant colonies were stained with Giemsa's solution. As shown in Fig. 4A, a significant decrease in number of drug-resistant colonies was observed in U2OS cells transfected with UNC5H4 expression plasmid relative to control cells, whereas UNC5H4 failed to show a significant effect on H1299 cells. Furthermore, UNC5H4-dependent induction of proteolytic cleavage of PARP was detected in U2OS cells, suggesting that UNC5H4-mediated decrease in number of drug-resistant colonies is attributed to the induction of apoptosis (Fig. 4B). Thus, it is likely that UNC5H4-mediated apoptosis is dependent on *p53* status.

To ask the functional significance of endogenous UNC5H4, we designed four siRNAs against UNC5H4 (#1, #2, #3 and #4). Among cell lines that we examined, osteosarcoma SAOS-2 cells express *UNC5H4* at the highest level (data not shown) and we used SAOS-2 cells to check the effectiveness of each of these siRNAs. Transfection of each of these siRNAs into SAOS-2 cells revealed that #1 and #3 siRNAs significantly down-regulate *UNC5H4* (Fig. 4C). Thus, we used #3 siRNA for further experiments. To address whether UNC5H4 could contribute to ADR-mediated apoptosis, U2OS cells were transfected with control siRNA or with #3 siRNA and exposed ADR. Forty-eight hours after ADR treatment, cells were analyzed for their cell cycle distributions by FACS. As shown in Fig. 4D, siRNA-mediated knockdown of UNC5H4 resulted in a decrease in number of cells with sub-G0/G1 DNA content relative to control cells, indicating that UNC5H4 plays an important role in the regulation of ADR-mediated apoptosis. Similar results were also obtained in U2OS cells transfected with #1 siRNA (data not shown).

Discussion

In the present study, we employed luciferase reporter assay and ChIP analysis to show that *UNC5H4* is a direct transcriptional target of p53 and its gene product has an apoptosis-inducing activity. Consistent with these results, ADR-mediated accumulation of p53 significantly correlates with transcriptional up-regulation of *UNC5H4* in U2OS cells. In contrast, ADR had undetectable effect on *UNC5H4* in p53-deficient H1299 cells. We have also found out several putative p53-binding sites in the 5′-upstream region of *UNC5H4*. Luciferase reporter assay demonstrated that these elements do not respond to exogenously expressed p53 (data not shown). Thus, we conclude that intronic p53-RE1 and p53-RE2 are genuine p53-responsive elements.

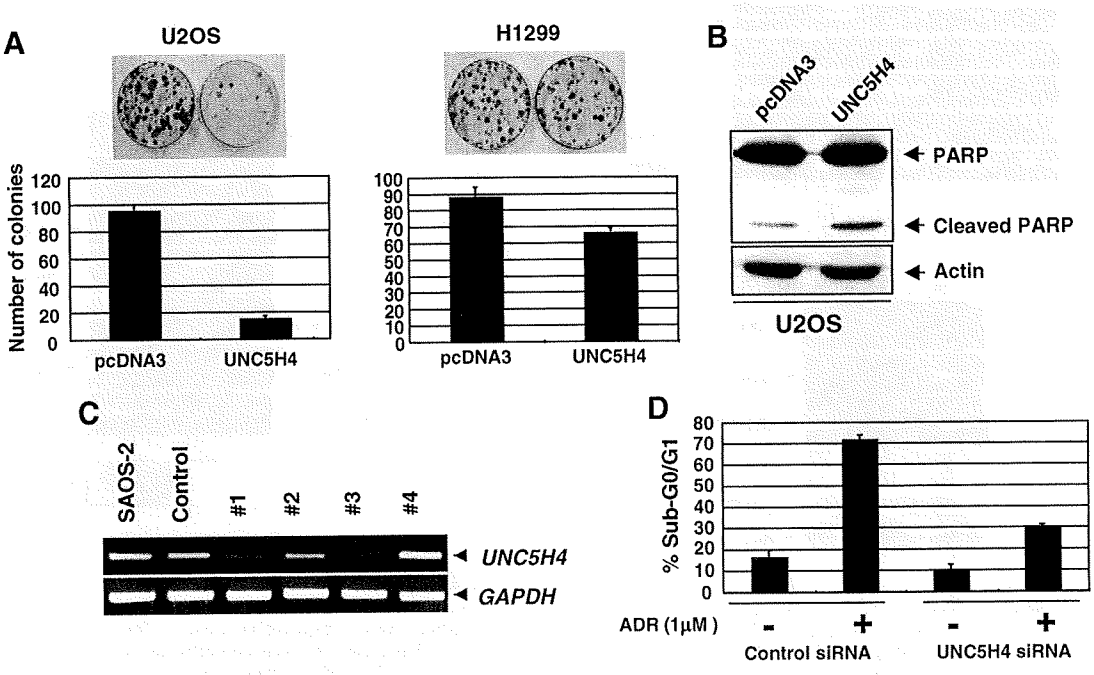

Fig. 4. UNC5H4-mediated apoptosis is dependent on p53. (A) Colony formation assay. U2OS and H1299 cells were transfected with the expression plasmid for UNC5H4. Forty-eight hours after transfection, cells were exposed to 400 μg/ml of G418 for two weeks. Drug-resistant colonies were then stained with Giemsa's solution. (B) Proteolytic cleavage of PARP. U2OS cells were transfected with the empty plasmid or with UNC5H4 expression plasmid. Forty-eight hours after transfection, cell lysates were prepared and processed for immunoblotting with anti-PARP antibody. (C) siRNA-mediated knockdown of UNC5H4. SAOS-2 cells were transfected with indicated siRNAs. Forty-eight hours after transfection, total RNA was prepared and subjected to RT-PCR. (D) siRNA-mediated knockdown of UNC5H4 renders U2OS cells resistant to ADR. U2OS cells were transfected with control siRNA or with siRNA against UNC5H4. Twenty-four hours after transfection, cells were treated with 1 μM of ADR. Forty-eight hours after ADR treatment, cells were stained with propidium iodide (PI) and their cell cycle distributions were analyzed by FACS.

Similar to the other UNC5H family members, UNC5H4 contains a canonical caspase cleavage site (413-DVID-416) [11] in its cytoplasmic region and enforced expression of UNC5H4 caused an apoptosis. Although it has been largely unknown how membrane UNC5H family proteins could transmit an apoptotic signal from cell surface to cytoplasm and/or nucleus, it is worth noting that UNC5H1–3 are cleaved by caspase-3 and treatment of cells with potent caspase inhibitor completely blocks UNC5H-mediated apoptosis [2], indicating that activated caspase-mediated proteolytic cleavage of cytoplasmic region of UNC5H including death domain plays an important role in the induction of apoptosis. Tanikawa et al. detected the cleaved fragment derived from UNC5H2 in cells infected with adenovirus encoding p53 [13]. Our preliminary results indicated that the cleaved fragment derived from UNC5H4 is detectable in both cytoplasm and nucleus of cells transfected with the expression plasmid for UNC5H4 (data not shown). Considering that UNC5H4-mediated induction of apoptosis is dependent on *p53* status, it is possible that functional interaction between p53 and cleaved fragment of UNC5H4 might take place in cell nucleus, and thereby amplifying p53-mediated apoptotic response. Further study should be required to address this issue.

Acknowledgments

We are grateful to Dr. H. Arakawa for valuable discussion. This work was supported in part by a Grant-in-Aid from the Ministry of Health, Labour and Welfare for the Third Term Comprehensive Control Research for Cancer, a Grant-in-Aid for Scientific Research on Priority Areas from the Ministry of Education, Culture, Sports, Science and Technology, Japan, a Grant-in-Aid for Scientific Research from Japan Society for the Promotion of Science, Uehara Memorial Foundation and Hisamitsu Pharmaceutical Co.

References

[1] P. Mehlen, S. Rabizadeh, S.J. Snipas, N. Assa-Munt, G.S. Salvesen, D.E. Bredesen, The DCC gene product induces apoptosis by a mechanism requiring receptor proteolysis, Nature 395 (1998) 801–804.
[2] F. Llambi, F. Causeret, E. Bloch-Gallego, P. Mehlen, Netrin-1 acts as a survival factor via its receptors UNC5H and DCC, EMBO J. 20 (2001) 2715–2722.
[3] P. Mehlen, D.E. Bredesen, The dependence receptor hypothesis, Apoptosis 9 (2004) 37–49.
[4] E.R. Fearon, K.R. Cho, J.M. Nigro, S.E. Kern, J.W. Simons, J.M. Ruppert, J.D. Oliner, K.W. Kinzler, B. Vogelstein, Identification of a chromosome 18q gene that is altered in colorectal cancers, Science 247 (1990) 49–56.
[5] E.R. Fearon, DCC: is there a connection between tumorigenesis and cell guidance molecules?, Biochim Biophys. Acta 1288 (1996) M17–M23.
[6] M. Tessier-Lavigne, C.S. Goodman, The molecular biology of axon guidance, Science 274 (1996) 1123–1133.
[7] E.D. Leonardo, I. Hinck, M. Masu, K. Keino-Masu, S.I. Ackerman, M. Tessier-Lavigne, Vertebrate homologues of *C. elegans* UNC-5 are candidate netrin receptors, Nature 386 (1997) 833–838.
[8] K. Hong, I. Hinck, M. Nishiyama, M.M. Poo, M. Tessier-Lavigne, E. Stein, A ligand-gated association between cytoplasmic domains of UNC5 and DCC family receptors converts netrin-induced growth cone attraction to repulsion, Cell 97 (1999) 927–941.
[9] N. Yokota, T.G. Mainprize, M.D. Taylor, T. Kohata, M. Loreto, S. Ueda, W. Dura, W. Grajkowska, J.S. Kuo, J.T. Rutka, Identification of differentially expressed and developmentally regulated genes in medulloblastoma using suppression subtraction hybridization, Oncogene 23 (2004) 3444–3453.
[10] K. Thiebault, L. Mazelin, L. Pays, F. Llambi, M.O. Joly, J.Y. Scoazec, J.C. Saurin, G. Romeo, P. Mehlen, The netrin-1 receptors UNC5H are putative tumor suppressors controlling cell death commitment, Proc. Natl. Acad. Sci. USA *100* (2003) 4173–4178.
[11] N.A. Thornberry, T.A. Rano, E.P. Peterson, D.M. Rasper, T. Timkey, M. Garcia-Calvo, V.M. Houtzager, P.A. Nordstrom, S. Roy, J.P. Vaillancourt, K.T. Chapmann, A combinatorial approach defines specificities of members of the caspase family and granzyme B. Functional relationships established for key mediators of apoptosis, J. Biol. Chem. 272 (1997) 17907–17911.
[12] M.E. Williams, P. Strickland, K. Watanabe, I. Hinck, UNC5H1 induces apoptosis via its juxtamembrane region through an interaction with NRAGE, J. Biol. Chem. 278 (2003) 17483–17490.
[13] C. Tanikawa, K. Matsuda, S. Fukuda, Y. Nakamura, H. Arakawa, *p53RDL1* regulates p53-dependent apoptosis, Nat. Cell Biol. 5 (2003) 216–223.
[14] F. Llambi, F. Calheiros-Lourenco, D. Gozuacik, C. Guix, L. Pays, G. Del Rio, Kimchi, P. Mehlen, The dependence receptor UNC5H2 mediates apoptosis through DAP-kinase, EMBO J. 24 (2005) 1192–1201.
[15] T. Reveh, G. Droguertt, M.S. Horwitz, R.A. DePinho, A. Kimchi, DAP kinase activates a p19ARF/p53-mediated apoptotic checkpoint to suppress oncogenic transformation, Nat. Cell Biol. 3 (2001) 1–7.
[16] T. Ichikawa, Y. Suenaga, T. Koda, T. Ozaki, A. Nakagawara, TAp63-dependent induction of growth differentiation factor 15 (*GDF15*) plays a critical role in the regulation of keratinocyte differentiation, Oncogene 27 (2008) 409–420.
[17] K.H. Vousden, X. Lu, Live or let die: the cell's response to p53, Nat. Rev. Cancer 2 (2002) 594–604.
[18] T. Miyashita, J.C. Reed, Tumor suppressor p53 is a direct transcriptional activator of the human *bax* gene, Cell 80 (1995) 293–299.

THE JOURNAL OF BIOLOGICAL CHEMISTRY VOL. 283, NO. 13, pp. 8555–8563, March 28, 2008

Inhibitory Role of Plk1 in the Regulation of p73-dependent Apoptosis through Physical Interaction and Phosphorylation*[S]

Received for publication, December 31, 2007 Published, JBC Papers in Press, January 3, 2008, DOI 10.1074/jbc.M710608200

Nami Koida[‡§], Toshinori Ozaki[‡], Hideki Yamamoto[‡], Sayaka Ono[¶], Tadayuki Koda[¶], Kiyohiro Ando[‡], Rintaro Okoshi[‡], Takehiko Kamijo[‡], Ken Omura[§], and Akira Nakagawara[‡1]

From the [‡]Division of Biochemistry, Chiba Cancer Center Research Institute, Chiba 260-8717, the [§]Department of Oral and Maxillofacial Surgery, Tokyo Medical and Dental University, Tokyo 113-8549, and [¶]Center for Functional Genomics, Hisamitsu Pharmaceutical Company, Incorporated, Chiba 260-8717, Japan

In response to DNA damage, p73 plays a critical role in cell fate determination. In this study, we have found that Plk1 (polo-like kinase 1) associates with p73, phosphorylates p73 at Thr-27, and thereby inhibits its pro-apoptotic activity. During cisplatin-mediated apoptosis in COS7 cells in which the endogenous p53 is inactivated by SV40 large T antigen, p73 was induced to accumulate in association with a significant down-regulation of Plk1. Consistent with these observations, Plk1 reduced the stability of the endogenous p73. Immunoprecipitation and *in vitro* pulldown assay demonstrated that p73 binds to the kinase domain of Plk1 through its NH_2-terminal region. Luciferase reporter assay and reverse transcription-PCR analysis revealed that Plk1 is able to block the p73-mediated transcriptional activation. Of note, kinase-deficient Plk1 mutant (Plk1(K82M)) retained an ability to interact with p73; however, it failed to inactivate the p73-mediated transcriptional activation, suggesting that kinase activity of Plk1 is required for the inhibition of p73. Indeed, *in vitro* kinase assay indicated that p73 is phosphorylated at Thr-27 by Plk1. Furthermore, small interference RNA-mediated knockdown of the endogenous Plk1 in p53-deficient H1299 cells resulted in a significant increase in the number of cells with sub-G_1 DNA content accompanied by the up-regulation of p73 and pro-apoptotic $p53^{AIP1}$ as well as the proteolytic cleavage of poly(ADP-ribose) polymerase. Thus, our present results suggest that Plk1-mediated dysfunction of p73 is one of the novel molecular mechanisms to inhibit the p53-independent apoptosis, and the inhibition of Plk1 might provide an attractive therapeutic strategy for cancer treatment.

p73 is one of newly identified *p53* tumor suppressor gene family members (*p53*, *p73*, and *p63*) that encodes a nuclear transcription factor (1–3). Like the other *p53* family members, *p73* encodes multiple isoforms, including TA (transactivating), with distinct COOH-terminal extensions arising from alternative splicing events and ΔN (nontransactivating) variants generated by alternative promoter usage (2–4). ΔNp73 has an oncogenic potential (5) and displays a dominant-negative behavior toward TAp73 as well as wild-type p53 (6). TAp73 transactivates overlapping set of p53-target genes implicated in the induction of cell cycle arrest and/or apoptosis, and plays an important role in the regulation of DNA damage response, which is closely linked to its DNA binding activity. The initial studies demonstrated that TAp73 does not induce enough to accumulate in response to DNA damage arising from UV exposure or actinomycin D treatment (1); however, it has been shown that, in response to certain subset of DNA-damaging agents, TAp73 accumulates in the cell nucleus and exerts its pro-apoptotic function (7).

Accumulating evidence suggests that TAp73 is regulated by post-translational modifications such as phosphorylation and acetylation. For example, TAp73 is stabilized in response to DNA damage such as cisplatin (CDDP)[2] treatment or exposure to γ-irradiation through the phosphorylation at Tyr-99 mediated by c-Abl (8–10). Ren *et al.* (11) demonstrated that protein kinase Cδ catalytic fragment phosphorylates TAp73 at Ser-289 in response to CDDP and thereby enhances its stability and activity. Further studies revealed that CDDP-mediated apoptosis is associated with phosphorylation of TAp73 at Ser-47 catalyzed by Chk1 (12). According to their results, Chk1-mediated phosphorylation of TAp73 resulted in an increase in its transcriptional activity. On the other hand, Gaiddon *et al.* (13) described that cyclin-dependent kinase phosphorylates TAp73 at Thr-86 and thereby reduces its transcriptional activity, suggesting that phosphorylation of TAp73 might not always convert a latent form of TAp73 to an active one. Additionally, several lines of evidence suggest that acetylation of TAp73 mediated by p300/CBP results in its activation (14). Constanzo *et al.* (15) reported that p300 has an ability to acetylate TAp73 at Lys-321, Lys-327, and Lys-331 in response to DNA damage in a c-Abl-dependent manner, and acetylated forms of TAp73 exert its pro-apoptotic function.

* This work was supported in part by a grant-in-aid from the Ministry of Health, Labor, and Welfare for Third Term Comprehensive Control Research for Cancer, a grant-in-aid for scientific research on priority areas from the Ministry of Education, Culture, Sports, Science, and Technology, Japan, a grant-in-aid for scientific research from Japan Society for the Promotion of Science, and a grant from Uehara Memorial Foundation. The costs of publication of this article were defrayed in part by the payment of page charges. This article must therefore be hereby marked "*advertisement*" in accordance with 18 U.S.C. Section 1734 solely to indicate this fact.

[S] The on-line version of this article (available at http://www.jbc.org) contains supplemental Figs. S1–S5.

[1] To whom correspondence should be addressed. Tel.: 81-43-264-5431; Fax: 81-43-265-4459; E-mail: akiranak@chiba-cc.jp.

[2] The abbreviations used are: CDDP, cisplatin; DAPI, 4, 6-diamidino-2-phenylindole; FACS, fluorescence-activated cell sorter; *GAPDH*, glyderaldehyde-3-phosphate dehydrogenase; GST, glutathione *S*-transferase; IB, immunoblotting; IP, immunoprecipitation; NMS, normal mouse serum; PARP, poly(ADP-ribose) polymerase; PBS, phosphate-buffered saline; RT, reverse transcription; siRNA, small interference RNA; GFP, green fluorescent protein.

Plk1 (Polo-like kinase 1) is a positive cell cycle regulator (16–18). Plk1 has an NH_2-terminal Ser/Thr protein kinase domain and tandem repeats of so-called "Polo-box motif" in its COOH-terminal region that might act as a phosphopeptide-binding domain (19). It has been shown that *Plk1* is overexpressed in a variety of human tumors as compared with their corresponding normal tissues (20, 21). Indeed, enforced expression of Plk1 in mouse fibroblasts causes oncogenic focus formation and promotes tumor growth in nude mice (22), suggesting that Plk1 has an oncogenic potential. In support with this notion, knockdown of the endogenous Plk1 induces G_2/M cell cycle arrest and/or apoptosis in various cell lines (23–25). Furthermore, it has been shown that Plk1 is inhibited in response to DNA damage in a mutated in ataxia telangiectasia (ATM) and ATM related kinase-dependent manner (26, 27), indicating that Plk1 is one of targets of DNA damage response. In this regard, we have found that Plk1 inhibits pro-apoptotic function of p53 through the physical interaction with it (20). Recently, Liu *et al.* (28) reported that Plk1 depletion promotes apoptosis of cancerous cells in a p53-independent manner. In this study, we have found that Plk1 has an ability to bind to and phosphorylate TAp73 at Thr-27, thereby inhibiting its transcriptional as well as pro-apoptotic activity.

EXPERIMENTAL PROCEDURES

Cell Lines and Transfection—African green monkey kidney COS7, human osteosarcoma SAOS-2, U2OS, and human cervical carcinoma HeLa cells were maintained in Dulbecco's modified Eagle's medium supplemented with 10% heat-inactivated fetal bovine serum (Invitrogen), 50 μg/ml penicillin, and 50 μg/ml streptomycin (Invitrogen). Human lung carcinoma H1299 cells were grown in RPMI 1640 medium supplemented with 10% heat-inactivated fetal bovine serum plus antibiotics mixture. These cells were cultured in a 5% CO_2 environment at 37 °C. Where indicated, cells were exposed to CDDP (Sigma). For transient transfection, COS7 and H1299 cells were transfected with the indicated combinations of the expression plasmids using Lipofectamine 2000 transfection reagent (Invitrogen) according to the manufacturer's instructions. pcDNA3 (Invitrogen) was used as a blank plasmid to balance the amount of DNA introduced in transient transfection.

RNA Extraction and RT-PCR—Total RNA was prepared from the indicated cells by using the RNeasy mini kit (Qiagen, Valencia, CA) according to the manufacturer's protocol and reverse-transcribed. The specific primers used were as follows: *p73α*, 5′-TCTGGAACCAGACAGCACCT-3′ and 5′-GTGCTGGACTGCTGGAAAGT-3′; $p21^{WAF1}$, 5′-ATGAAATTCACCCCCTTTCC-3′ and 5′-CCCTAGGCTGTGCTCACTTC-3′; *BAX*, 5′-TTTGCTTCAGGGTTTCATCC-3′ and 5′-CAGTTGAAGTTGCCGTCAGA-3′; *MDM2*, 5′-ACTTGAGCCGAGGAGTTCAA-3′ and 5′-TTGCTCTGTCACCTGGACTG-3′; *Plk1*, 5′-ATCACCTGCCTGACCATTCCACCAAGG-3′ and 5′-AATTGCGGAAATATTTAAGGAGGGTGATCT-3′; $p53^{AIP1}$, 5′-GATCTTCCTCTGAGGCGAGCT-3′ and 5′-TTACCCAGCCAGGTGTGTGT-3′; and *GAPDH*, 5′-ACCTGACCTGCCGTCTAGAA-3′ and 5′-TCCACCACCCTGTTGCTGTA-3′. The expression of *GAPDH* was measured as an internal control.

Immunoblotting—Whole cells lysates were prepared by incubating cells in lysis buffer containing 25 mM Tris-HCl, pH 8.0, 137 mM NaCl, 2.7 mM KCl, 1% Triton X-100 and a commercial protease inhibitor mixture (Sigma) for 30 min on ice and subjected to a brief sonication for 10 s at 4 °C followed by centrifugation at 15,000 rpm at 4 °C for 10 min to remove insoluble materials. The protein concentrations were measured using the Bradford protein assay according to the manufacturer's instructions (Bio-Rad). The equal amounts of protein (50 μg) were separated by 10% SDS-PAGE and electrophoretically transferred onto polyvinylidene difluoride membranes (Immobilon-P, Millipore, Bedford, MA). The transferred membranes were blocked with Tris-buffered saline containing 5% nonfat dry milk and 0.1% Tween 20 at 4 °C overnight. After blocking, the membranes were incubated with monoclonal anti-p73 (Ab-4; NeoMarkers, Fremont, CA), monoclonal anti-FLAG (M2; Sigma), monoclonal anti-Plk1 (PL2 and PL6; Zymed Laboratories Inc.), monoclonal anti-PARP (F-2; Santa Cruz Biotechnology, Santa Cruz, CA), polyclonal anti-p300 (H-272; Santa Cruz Biotechnology), or with polyclonal anti-actin (20–33; Sigma) antibody for 1 h at room temperature. After incubation with primary antibodies, the membranes were incubated with horseradish peroxidase-coupled goat anti-mouse or anti-rabbit IgG secondary antibody (Cell Signaling, Beverly, MA) for 1 h at room temperature. Immunoblots were visualized by ECL detection reagents according to the manufacturer's instructions (Amersham Biosciences).

Immunoprecipitation—HeLa cells were treated with CDDP at a final concentration of 20 μM. Twenty-four hours after CDDP treatment, whole cell lysates (1 mg of protein) were precleared with 30 μl of protein G-Sepharose beads and used for immunoprecipitation with the appropriate antibodies. After the addition of 30 μl of protein G-Sepharose beads, incubations were continued for additional 2 h at 4 °C. The beads were then collected by centrifugation and washed three times with the lysis buffer. The precipitated proteins were analyzed by 10% SDS-PAGE and immunoblotting with the appropriate antibodies as described.

GST Pulldown Assay—cDNA fragments encoding the indicated deletion mutants of p73α were generated by PCR-based strategy, and subcloned into GST fusion protein expression plasmid pGEX-4T-3 (Amersham Biosciences). GST and GST-p73α fusion proteins were expressed and purified by glutathione-Sepharose beads (Amersham Biosciences). FLAG-Plk1 was radiolabeled *in vitro* by using TnT QuickCoupled transcription/translation system (Promega, Madison, WI) in the presence of [^{35}S]methionine and incubated with GST or GST-p73α deletion mutants for 2 h at 4 °C. After the addition of 30 μl of glutathione-Sepharose beads into the reaction mixture, incubations were continued for 1 h at 4 °C. The beads were collected by centrifugation and washed three times with binding buffer containing 50 mM Tris-HCl, pH 7.5, 150 mM NaCl, 0.1% Nonidet P-40, and 1 mM EDTA. The ^{35}S-labeled bound proteins were eluted by 2× SDS sample buffer and separated by 10% SDS-PAGE. After electrophoresis, the gel was dried and exposed to an x-ray film with an intensifying screen.

Indirect Immunofluorescence Staining—HeLa cells were fixed in 3.7% formaldehyde for 30 min at room temperature,

permeabilized in 0.2% Triton X-100 for 5 min at room temperature, and then blocked with 3% bovine serum albumin in PBS for 1 h at room temperature. After blocking, cells were washed in PBS and incubated with polyclonal anti-p73 antibody (H-79; Santa Cruz Biotechnology) and monoclonal anti-Plk1 antibody for 1 h at room temperature, followed by the incubation with fluorescein isothiocyanate-conjugated anti-rabbit IgG and rhodamine-conjugated anti-mouse IgG (Invitrogen) for 1 h at room temperature. Cell nuclei were stained with DAPI.

Flow Cytometry—After transfection, both floating and attached cells were collected by low speed centrifugation, washed in PBS, and fixed in 70% ethanol at −20 °C overnight. The cells were then stained with propidium iodide (50 μg/ml) in the presence of 50 μg/ml RNase A for 30 min at room temperature. The DNA content indicated by propidium iodide staining was analyzed by FACSCalibur flow cytometer (BD Biosciences).

Luciferase Reporter Assay—p53-deficient H1299 cells were plated in 12-well plates at a density of 50,000 cells/well and transiently co-transfected with a constant amount of a luciferase reporter construct driven by p53/p73-responsive element derived from $p21^{WAF1}$, *Mdm2*, or *Bax* promoter, *Renilla* luciferase expression plasmid (pRL-TK), and the HA-p73α expression plasmid together with or without the increasing amounts of the expression plasmid for Plk1. Forty-eight hours after transfection, cells were lysed, and their luciferase activities were measured by dual luciferase reporter assay system (Promega). The firefly luminescence signal was normalized based on the *Renilla* luminescence signal. Each experiment was performed at least three times in triplicate.

Apoptotic Assay—H1299 cells were transfected with the indicated combinations of the expression plasmids. Forty-eight hours after transfection, cells were washed in PBS, fixed in 3.7% formaldehyde for 1 h at room temperature, and then permeabilized with 0.1% Triton X-100 for 5 min on ice. The cell nuclei were stained by DAPI. The number of GFP-positive cells with apoptotic nuclei was counted.

Construction of Mutant Forms of GST-p73α-(1–130)—To identify possible phosphorylation site(s) of p73α mediated by Plk1, the T27A mutation was introduced into the GST-p73α-(1–130) using PfuUltra™ high fidelity DNA polymerase (Stratagene, La Jolla, CA) according to the manufacturer's instructions. Details are available upon request. Nucleotide sequences of the PCR products were determined to verify the presence of the desired mutation and the absence of random mutations.

In Vitro Kinase Reaction—To identify the possible Thr residue(s) of p73α that could be phosphorylated by Plk1, we used CycLex Polo-like kinase 1 assay kit (CycLex, Nagano, Japan) (29). In brief, the purified Plk1 was added to the reaction mixture containing 50 μM ATP and polyclonal anti-phospho-Thr antibody and incubated for 30 min at room temperature. After the incubation, horseradish peroxidase-conjugated anti-rabbit IgG secondary antibody was mixed with the reaction mixture and incubated for 30 min at room temperature. Finally, GST or the indicated GST-p73α deletion mutants dissolved in substrate solution were added into the reaction mixture and incubated for 5 min at room temperature, followed by the measurement of absorbance in each well using a spectrophotometric plate reader at dual wavelength of 450/540 nm. As a positive control, we used protein X that was supplied by the manufacturer.

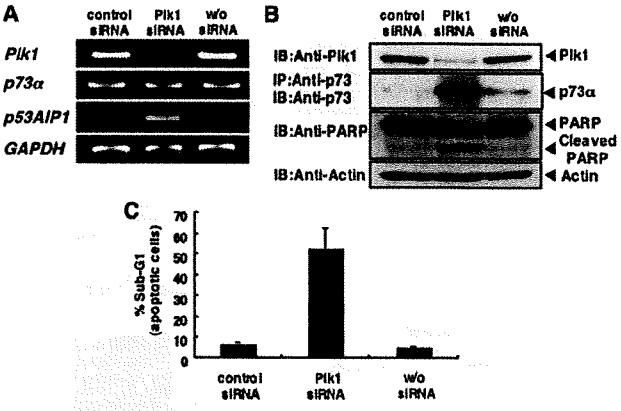

FIGURE 1. **siRNA-mediated knockdown of Plk1 induces apoptosis in p53-deficient H1299 cells.** *A*, siRNA-mediated knockdown of the endogenous *Plk1*. H1299 cells were transfected with control siRNA or with Plk1 siRNA (Plk1 siRNA). Forty-eight hours after transfection, total RNA was prepared and subjected to RT-PCR to examine the expression levels of *Plk1*, *p73α*, and $p53^{AIP1}$. *GAPDH* was used as an internal control. *B*, immunoblotting analysis. H1299 cells were transfected as in *A*. Forty-eight hours after transfection, whole cell lysates were prepared and processed for immunoblotting (*IB*) with the indicated antibodies. For the detection of the endogenous p73α, whole cell lysates were subjected to immunoprecipitation (IP) with anti-p73 antibody followed by IB with anti-p73 antibody. Actin expression served as a control for equal loading of proteins in each lane. *C*, FACS analysis. H1299 cells were transfected as in *A*. Forty-eight hours after transfection, attached and floating cells were harvested, stained with PI, and their cell cycle distributions examined by flow cytometry.

RNA Interference—To knock down the endogenous Plk1, H1299 cells were transiently transfected with the chemically synthesized siRNA targeting Plk1 or with the control siRNA (Dharmacon, Chicago) using Lipofectamine™ RNAiMAX (Invitrogen) according to the manufacturer's recommendations. Total RNA and whole cell lysates were prepared 48 h after transfection.

RESULTS

siRNA-mediated Knockdown of Plk1 Results in a Massive Apoptosis—To ask whether Plk1 could protect cells from p53-independent apoptosis, p53-deficient human lung carcinoma H1299 cells were transfected with control siRNA or with siRNA against Plk1. As shown in Fig. 1*A*, *Plk1* was successfully knocked down under our experimental conditions. The expression levels of *p73α* remained unchanged. Of note, the expression levels of pro-apoptotic $p53^{AIP1}$, which is one o the p53/p73 target genes, were significantly induced in Plk1-knocked down cells. Immunoblot analysis clearly demonstrated that the proteolytic cleavage of PARP, which is one of the substrates of the activated caspase-3 (30), is observed in Plk1-knocked down cells in association with a significant induction of pro-apoptotic p73α (Fig. 1*B*). FACS analysis revealed that siRNA-mediated knockdown of the endogenous Plk1 causes a remarkable increase in number of cells with sub-G_1 DNA content relative to control cells (Fig. 1*C*). Similar results were also obtained in H1299 cells transfected with other siRNAs against Plk1 (data not shown), suggesting that Plk1 might have an inhibitory effect on p73-mediated apoptosis. Similar results were also obtained

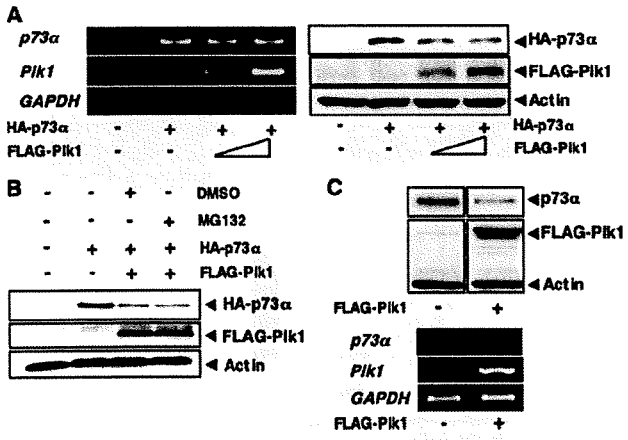

FIGURE 2. **Plk1 promotes proteolytic degradation of p73 in a proteasome-independent manner.** *A*, enforced expression of Plk1 reduces the expression levels of p73. H1299 cells were co-transfected with the constant amount of HA-p73α (0.5 μg) expression plasmid together with or without the expression plasmid for FLAG-Plk1 (0.5 and 1.0 μg). Forty-eight hours after transfection, total RNA and whole cell lysates were prepared and subjected to RT-PCR (*left panels*) and IB with the indicated antibodies (*right panels*), respectively. *B*, H1299 cells were transfected with the expression plasmid for HA-p73α alone or with HA-p73α (0.5 μg) plus FLAG-Plk1 (0.5 μg) expression plasmids. Forty-eight hours after transfection, cells were treated with *DMSO* or with 20 μM of MG-132 for 6 h. Whole cell lysates were then extracted and subjected to IB with the indicated antibodies. *C*, H1299 cells were transfected with pcDNA3 or with FLAG-Plk1 expression plasmid. Forty-eight hours after transfection, whole cell lysates and total RNA were prepared and subjected to IP with anti-p73 antibody followed by IB with anti-p73 antibody (*upper panels*) and RT-PCR (*lower panels*), respectively. Actin was used as a loading control, and *GAPDH* was used as an internal control.

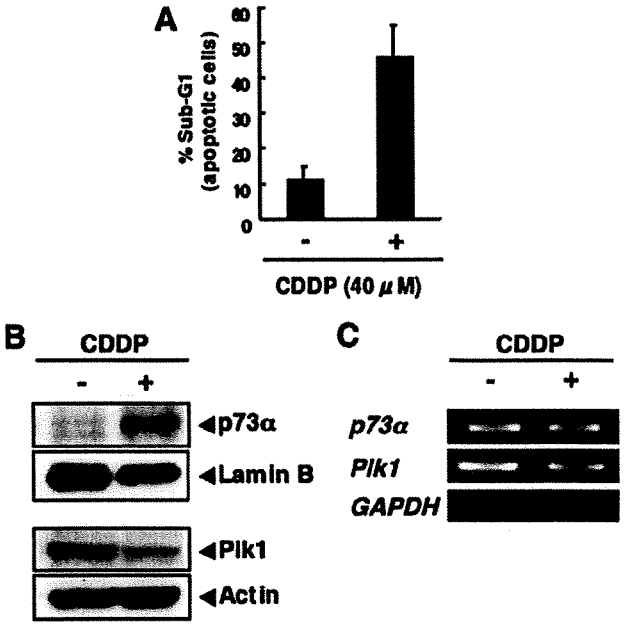

FIGURE 3. **Inverse relationship between the endogenous expression levels of p73 and Plk1 in response to CDDP.** *A–C*, COS7 cells were treated with 40 μM of CDDP or left untreated. Forty-eight hours after the treatment, floating and attached cells were collected, stained with PI, and their cell cycle distributions analyzed by flow cytometry (*A*). COS7 cells were treated with 40 μM of CDDP or left untreated. Forty-eight hours after the treatment, nuclear (*upper panels*) and whole cell lysates (*lower panels*) were prepared and subjected to IB with the indicated antibodies (*B*). Total RNA was also prepared and analyzed by RT-PCR (*C*).

in p53-proficient U2OS cells as well as p53-deficient SAOS-2 cells (supplemental Fig. S1). Thus, it is likely that siRNA-mediated knockdown of the endogenous Plk1 induces apoptosis regardless of *p53* status.

These findings showing that siRNA-mediated knockdown of Plk1 leads to a significant induction of the endogenous p73α at protein level prompted us to examine whether Plk1 could affect the protein stability of p73. For this purpose, H1299 cells were co-transfected with the constant amount of the expression plasmid for HA-p73α together with or without the increasing amounts of FLAG-Plk1 expression plasmid. As shown in Fig. 2*A*, *left panel*, Plk1 had undetectable effect on the expression levels of *p73α* mRNA. On the other hand, immunoblotting analysis revealed that Plk1 reduces the amounts of HA-p73α (Fig. 2*A*, *right panel*). Intriguingly, Plk1-mediated reduction of HA-p73α was not recovered in the presence of proteasome inhibitor MG-132 (Fig. 2*B*). Similar results were also obtained in cells exposed to lactacystin (data not shown). In addition, enforced expression of FLAG-Plk1 significantly reduced the amounts of the endogenous p73α at protein level but not at the mRNA level (Fig. 2*C*).

As described previously (31), CDDP treatment led to a stabilization of the endogenous p73α in COS7 cells, whereas the endogenous Plk1 was down-regulated in response to CDDP accompanied by the induction of apoptosis (Fig. 3, *A–C*), indicating that there exists an inverse relationship between the expression levels of Plk1 and p73α in response to CDDP and that Plk1 might promote proteolytic degradation of p73α in a proteasome-independent manner. Furthermore, enforced expression of Plk1 decreased the sensitivity to CDDP in association with the reduction of CDDP-mediated proteolytic cleavage of PARP (supplemental Fig. S2).

Plk1 Inhibits p73-mediated Transcriptional Activation and Pro-apoptotic Function—To address whether Plk1 could suppress the transcriptional activity of p73, we performed the luciferase reporter assays. H1299 cells were co-transfected with the constant amount of the expression plasmid for HA-p73α, the luciferase reporter construct carrying p53/p73-responsive $p21^{WAF1}$, *BAX*, or *MDM2* promoter, and *Renilla* luciferase cDNA (pRL-TK) together with or without the increasing amounts of FLAG-Plk1 expression plasmid. As shown in Fig. 4, *A–C*, enforced expression of FLAG-Plk1 significantly reduced the luciferase activities driven by the indicated promoters in a dose-dependent manner. Consistent with these results, HA-p73α-mediated up-regulation of the endogenous $p21^{WAF1}$, *BAX*, and *MDM2* mRNAs was abrogated by FLAG-Plk1 (Fig. 4*D*), suggesting that Plk1 has an ability to repress the transcriptional activity of p73α.

To examine a possible effect of Plk1 on pro-apoptotic activity of p73, we carried out apoptotic assay. H1299 cells were co-transfected with the indicated combinations of the expression plasmids. Consistent with the previous observations (32), HA-p73α alone increased number of cells with apoptotic nuclei (Fig. 5*A*). As expected, FLAG-Plk1 had an ability to decrease GFP-positive cells with apoptotic nuclei caused by exogenous expression of HA-p73α. In accordance with these results, FACS analysis demonstrated that HA-p73α-mediated increase in

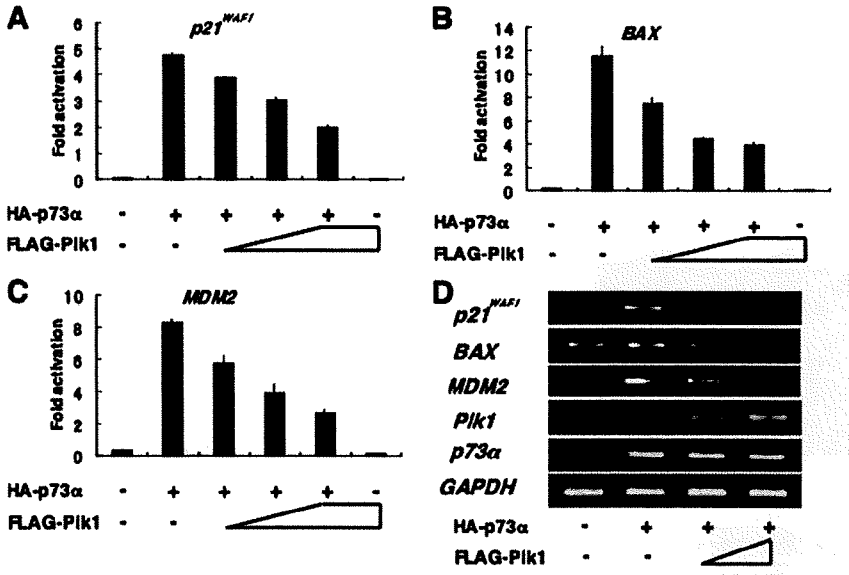

FIGURE 4. **Plk1 represses the p73-mediated transcriptional activation.** *A–C*, H1299 cells (5×10^4 cells) were co-transfected with the constant amount of HA-p73α expression plasmid (25 ng), 100 ng of p53/p73-responsive luciferase reporter construct bearing $p21^{WAF1}$ (*A*), *BAX* (*B*), or *MDM2* (*C*) promoter and 10 ng of *Renilla* luciferase reporter plasmid (pRL-TK) in the presence or absence of the increasing amounts of FLAG-Plk1 expression plasmid (50, 100, and 200 ng). To standardize the amounts of plasmid DNA per transfection, pcDNA3 was added to yield a total of 510 ng of plasmid. Forty-eight hours after transfection, cells were lysed, and their luciferase activities were measured. Data were normalized and presented as mean values ± S.D. of three independent experiments. *D*, RT-PCR analysis. H1299 cells were co-transfected with the constant amount of HA-p73α together with or without the increasing amounts of FLAG-Plk1 expression plasmid. Forty-eight hours after transfection, total RNA was prepared and analyzed for the expression levels of $p21^{WAF1}$, *BAX*, and *MDM2* by RT-PCR. Amplification of *GAPDH* serves as an internal control.

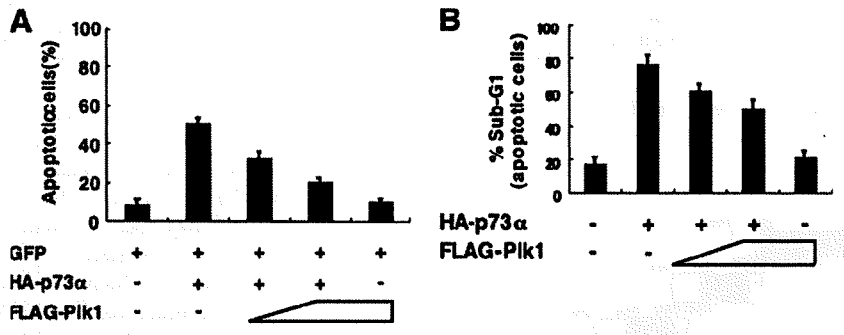

FIGURE 5. **Plk1 inhibits the pro-apoptotic activity of p73.** *A*, apoptotic assay. H1299 cells were seeded at a density of 2×10^5 cells/6-well tissue culture plate and allowed to attach overnight. Next day, cells were co-transfected with the constant amount of GFP (100 ng) and HA-p73α (900 ng) expression plasmids together with or without the increasing amounts of FLAG-Plk1 expression plasmid (500 and 1000 ng). Total amount of plasmid DNA was kept constant (2 μg) with pcDNA3. Forty-eight hours after transfection, cells were fixe, and cell nuclei were stained with DAPI. The percentages of GFP-positive cells with apoptotic nuclei were plotted. *B*, FACS analysis. H1299 cells were co-transfected with the constant amount of the expression plasmid encoding HA-p73α (250 ng) together with or without the increasing amounts of FLAG-Plk1 expression plasmid (100 or 200 ng). Forty-eight hours after transfection, attached and floating cells were collected, stained with PI, and their cell cycle distributions analyzed by flow cytometry.

number of cells with sub-G_1 DNA content is inhibited by co-expression with FLAG-Plk1 in a dose-dependent manner (Fig. 5*B*), indicating that Plk1 suppresses the p73α-mediated apoptotic cell death.

Interaction between Plk1 and p73 in Cells—To address whether Plk1 could associate with p73 in cells, we examined their subcellular distributions in response to CDDP. Human cervical carcinoma HeLa cells were treated with CDDP or left untreated for 24 h. Immunofluorescence microscopy demonstrated that the endogenous p73α is detectable in cell nucleus regardless of CDDP treatment (Fig. 6*A*). It was worth noting that the endogenous Plk1 localizes both in the cytoplasm and cell nucleus in the absence of CDDP, whereas CDDP treatment induces the nuclear accumulation of Plk1. Merged images revealed that Plk1 is largely co-localized with p73α in the cell nucleus in response to CDDP. Under our experimental conditions, immunofluorescence staining without primary antibodies did not show any positive signals (data not shown). These observations suggest that Plk1 might interact with p73 in cells exposed to CDDP.

To further confirm this notion, we performed immunoprecipitation experiments. HeLa cells were exposed to CDDP for 24 h, and whole cell lysates were immunoprecipitated with normal mouse serum (NMS) or with anti-p73 antibody followed by immunoblotting with anti-Plk1 antibody. As shown in Fig. 6*B*, *left panels*, the anti-p73 immunoprecipitates contained the endogenous Plk1. Reciprocal experiments demonstrated that p73 is co-immunoprecipitated with the endogenous Plk1 (Fig. 6*B*, *right panels*). Similar results were also obtained in the co-immunoprecipitation experiments using exogenous materials (supplemental Fig. S3). These observations strongly suggest that Plk1 interacts with p73α in cells.

To identify the essential region(s) of p73α required for the interaction with Plk1, we carried out *in vitro* pulldown assays. The indicated GST-p73α deletion mutants (Fig. 7*A*) were purified by glutathione-Sepharose beads (Fig. 7*B*). Each of these GST fusion proteins were incubated with the radiolabeled FLAG-Plk1, which was generated by *in vitro* transcription/translation system in the presence of [^{35}S]methionine. As clearly shown in Fig. 7*C*, the radiolabeled FLAG-Plk1 was efficiently pulled down by GST-p73α-(1–130) but not by the remaining GST fusion proteins, implying that the region between amino acid residues 63 and 113 of p73α is important for the interaction with Plk1.

In addition, we sought to determine the region of Plk1 required for the complex formation with p73α. To this end, we

generated the indicated Plk1 deletion mutants labeled with [^{35}S]methionine (Fig. 8*A*). These deletion mutants were incubated with GST-p73α-(1–130) (Fig. 8*B*). As shown in Fig. 8*C*, FLAG-Plk1-(1–401), FLAG-Plk1-(1–329), and FLAG-Plk1-(1–218) retained an ability to associate with GST-p73α-(1–130), whereas FLAG-Plk1-(1–98) failed to interact with GST-p73α-(1–130). These results indicated that the region between amino acid residues 99 and 218, including a part of the kinase domain of Plk1, is essential for the interaction with p73α.

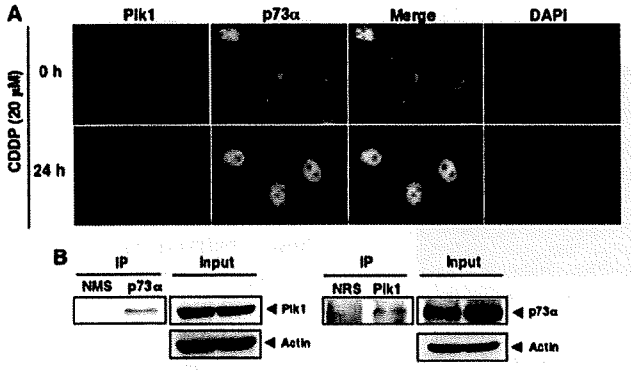

FIGURE 6. **Interaction between Plk1 and p73 in cells.** *A*, nuclear co-localization of Plk1 with p73 in response to CDDP. HeLa cells were treated with 20 μM CDDP (*lower panels*) or left untreated (*upper panels*). Twenty-four hours after the treatment cells were simultaneously probed with polyclonal anti-p73 antibody and monoclonal anti-Plk1 antibody for 1 h at room temperature. After extensive washing in PBS, cells were incubated with rhodamine-conjugated anti-mouse IgG (*red*) and fluorescein isothiocyanate-conjugated anti-rabbit IgG (*green*). Cell nuclei were stained with DAPI (*blue*). Merged images indicate the nuclear co-localization of Plk1 with p73α (*yellow*). *B*, immunoprecipitation. HeLa cells were exposed to 20 μM CDDP. Twenty-four hours after CDDP treatment, whole cell lysates were IP with NMS or with anti-p73 antibody followed by IB with anti-Plk1 antibody (*left panel*). Input lysates were analyzed by IB with the indicated antibodies. Reciprocal experiments are shown in the *right panels*.

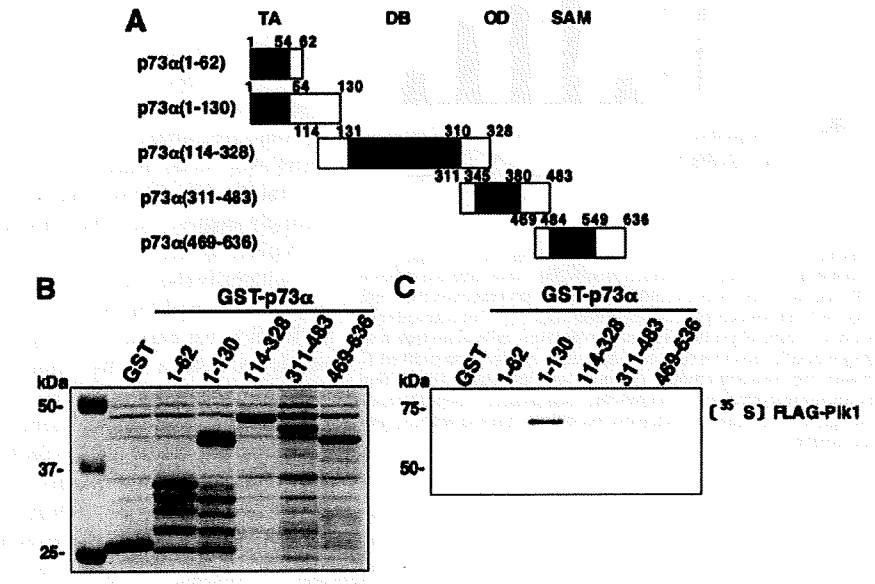

FIGURE 7. **NH_2-terminal small domain of p73 is required for the interaction with Plk1.** *A*, domain structure of wild-type p73α and schematic representation of GST-tagged p73α deletion mutants. *TA*, transactivation domain; *DB*, DNA-binding domain; *OD*, oligomerization domain; *SAM*, sterile α-motif domain. *Numbers* indicate amino acid positions. *B*, GST and GST-p73α fusion proteins were purified by glutathione-Sepharose beads and separated by 10% SDS-PAGE followed by Coomassie Brilliant Blue staining. *C*, *in vitro* pulldown assay. Equal amount of radiolabeled FLAG-Plk1 was incubated with GST or with the indicated GST-p73α fusion proteins. After incubation, GST or GST-p73α fusion proteins were recovered by glutathione-Sepharose beads, and bound materials were resolved by 10% SDS-PAGE followed by autoradiography.

Kinase Activity of Plk1 Is Required for the Inhibition of p73 Function—To examine whether the kinase activity of Plk1 could be necessary for the inhibition of p73 function, we tested a possible effect of the kinase-deficient mutant form of Plk1 (Plk1(K82M)) (20) on p73α. For this purpose, we first examined whether Plk1(K82M) could interact with p73α in cells. COS7 cells were co-transfected with the expression plasmids encoding HA-p73α and FLAG-Plk1(K82M). Forty-eight hours after transfection, whole cell lysates were immunoprecipitated with NMS or with anti-FLAG antibody followed by immunoblotting with anti-p73 or with anti-FLAG antibody. As seen in Fig. 9*A*, *left panels*, HA-p73α was co-immunoprecipitated with FLAG-Plk1(K82M). Similarly, the anti-p73 immunoprecipitates contained FLAG-Plk1(K82M) (Fig. 9*A*, *right panels*). These results suggest that the kinase-deficient mutant form of Plk1 retains an ability to interact with p73 in cells.

To further examine the effect of the kinase activity of Plk1 on p73 function, we performed luciferase reporter assays. H1299 cells were co-transfected with the constant amount of the expression plasmid for HA-p73α, luciferase reporter construct bearing p53/p73-responsive *p21^{WAF1}*, *BAX*, or *MDM2* promoter, and *Renilla* luciferase cDNA along with or without the increasing amounts of FLAG-Plk1(K82M). As shown in Fig. 9, *B–D*, FLAG-Plk1(K82M) had negligible effect on the transcriptional activity of HA-p73α. In contrast to wild-type Plk1, enforced expression of FLAG-Plk1(K82M) in H1299 cells had marginal effect on the expression levels of the endogenous p73α (supplemental Fig. S4). Collectively, these results indicate that kinase activity of Plk1 is required for the inhibition of p73 function.

Plk1 Phosphorylates p73 in Vitro—To address whether Plk1 could phosphorylate p73, we performed *in vitro* kinase reaction (29). To this end, we employed a CycLex Plk1 assay kit. As a positive control, we used protein X, which was provided by the manufacturer. According to the manufacturer's instructions, the active form of Plk1 was incubated with anti-phospho-Thr antibody, and then substrate proteins, including protein X, GST, or the indicated GST-p73α fusion proteins (Fig. 10*A*) were added to the reaction mixture. After the incubation, horseradish peroxidase-conjugated secondary antibody was mixed with the reaction mixtures. As shown in Fig. 10*B*, *yellow* color was observed in the reaction mixtures containing protein X, GST-p73α-(1–62), and GST-p73α-(1–130). Fig. 10*C* shows the results of quantification of the reactions, suggesting that Plk1 might phosphorylate Thr residue(s)

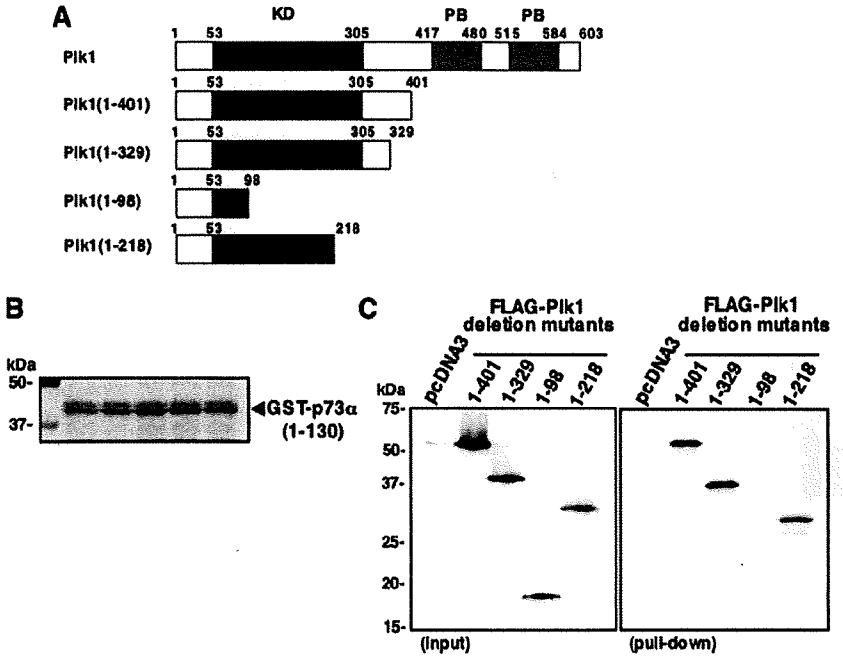

FIGURE 8. **Kinase domain of Plk1 is essential for the interaction with p73.** *A*, schematic drawing of wild-type Plk1 and its deletion mutants. *KD*, kinase domain; *PB*, polo-box domain. *B*, Coomassie Brilliant Blue staining of GST-p73α-(1–130) used for this study. *C*, *in vitro* pulldown assay. Equal amount of GST-p73α-(1–130) was incubated with radiolabeled FLAG-Plk1 deletion mutants (*left panel*). After incubation, GST-p73α-(1–130) was precipitated by glutathione-Sepharose beads, and bound materials were separated by SDS-PAGE followed by autoradiography.

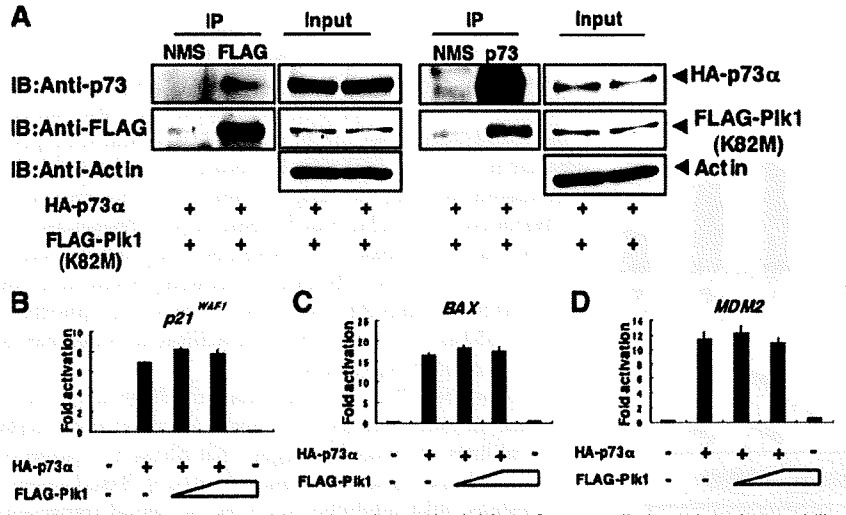

FIGURE 9. **Kinase activity of Plk1 is required for the inhibition of p73.** *A*, Plk1(K82M) retains an ability to interact with p73 in cells. COS7 cells were transiently co-transfected with the expression plasmids for HA-p73α and FLAG-Plk1(K82M). Forty-eight hours after transfection, whole cell lysates were prepared and subjected to IP with NMS or with anti-FLAG antibody. The immunoprecipitates were analyzed by IB with anti-p73 (*1st panel*) or with anti-FLAG (*2nd panel*) antibody. Input lysates were processed for IB with the indicated antibodies. *Right panels* show the results of the reciprocal experiments. *B–D*, luciferase reporter assay. H1299 cells were transiently co-transfected with the constant amount of HA-p73α expression plasmid (25 ng), 100 ng of luciferase reporter construct carrying p53/p73-responsive element derived from $p21^{WAF1}$ (*B*), *Bax* (*C*), or *MDM2* (*D*) promoter and 10 ng of pRL-TK together with or without the increasing amounts of the expression plasmid for FLAG-Plk1(K82M) (50 and 100 ng). Forty-eight hours after transfection, cells were lysed and their luciferase activities determined. Firefly luminescence signal was normalized based on the *Renilla* luminescence signal. Results were shown as fold induction of the firefly luciferase activity compared with control cells transfected with the empty plasmid alone.

within the region between amino acid residues 1 and 130 of p73α.

As described previously (33), a sequence (D/E)*X*(S/T)ψ*X*(D/E) (where *X* is any amino acid; ψ is hydrophobic amino acid) was identified as a consensus motif for Plk1-dependent phosphorylation. During the search for a putative phosphorylation site(s) targeted by Plk1 within the amino acid sequence of p73α (residues 1–130), we found out a related motif (^{25}DSTYFD^{30}) was in the NH_2-terminal portion of p73α. To further confirm whether Thr-27 of p73α could be phosphorylated by Plk1, we generated a mutant form of GST-p73α-(1–130), termed T27A, where Thr-27 was substituted to Ala. Purified GST fusion proteins (Fig. 11*A*) were subjected to the *in vitro* kinase reaction. As shown in Fig. 11, *B* and *C*, the amino acid substitution resulted in a significant reduction of Plk1-mediated phosphorylation level of GST-p73α-(1–130). Consistent with these results, GST-p73α-(1–130) and S48A mutant were strongly radiolabeled in the presence of Plk1, whereas T27A mutant was labeled to a lesser degree (Fig. 11*D*), indicating that Thr-27 of p73α is at least one of the phosphorylation sites targeted by Plk1. Taken together, our current results have exposed a novel molecular mechanism behind Plk1-mediated protection of cells from p73-dependent apoptosis.

DISCUSSION

In this study, we have found for the first time that p73 plays a crucial role in the induction of massive apoptosis in p53-deficient cells caused by siRNA-mediated depletion of the endogenous Plk1. Thus, it is likely that Plk1 protects p53-deficient cells from p73-mediated apoptosis. In this connection, inhibition of Plk1 function might provide a novel therapeutic strategy to treat tumors with *p53* mutation.

We have previously demonstrated that Plk1 interacts with p53 and suppresses its transcriptional as well as pro-apoptotic activity (20). According to our previous results,